Accepted Manuscript

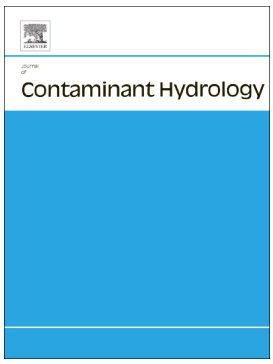

Competitive transport processes of chloride, sodium, potassium, and ammonium in fen peat

Colin P.R. McCarter, Tobias K.D. Weber, Jonathan S. Price

PII: S0169-7722(18)30112-8
DOI: doi:10.1016/j.jconhyd.2018.08.004
Reference: CONHYD 3414

To appear in: *Journal of Contaminant Hydrology*

Received date: 11 April 2018
Revised date: 1 August 2018
Accepted date: 11 August 2018

Please cite this article as: Colin P.R. McCarter, Tobias K.D. Weber, Jonathan S. Price , Competitive transport processes of chloride, sodium, potassium, and ammonium in fen peat. Conhyd (2018), doi:10.1016/j.jconhyd.2018.08.004

Competitive Transport Processes of Chloride, Sodium, Potassium, and Ammonium in Fen Peat

Colin P.R. McCarter[1†], Tobias K.D. Weber[2], and Jonathan S. Price[3]

[1] Dep. of Geography and Environmental Management, University of Waterloo, 200 University Ave West, Waterloo, ON, Canada N2L 3G1, Canada. ORCID: https://orcid.org/0000-0002-7308-0369,

[2] Institute for Soil Science and Land Evaluation, Biogeophysics, University of Hohenheim, Emil-Wolff-Straße 27, DE-70599 Stuttgart, Germany. ORCID: https://orcid.org/0000-0002-3448-5208

[3] Dep. of Geography and Environmental Management, University of Waterloo, 200 University Ave West, Waterloo, ON, Canada N2L 3G1, Canada.

Corresponding author: Colin McCarter (colin.mccarter@utoronto.ca)

†Currently at: Department of Physical and Environmental Sciences, University of Toronto Scarborough, 1265 Military Trail, Scarborough, M1C 1A4, Canada.

Abstract

There is sparse information on reactive solute transport in peat; yet, with increasing development of peatland dominated landscapes, purposeful and accidental contaminant releases will occur, so it is important to assess their mobility. Previous experiments with peat have only evaluated single-component solutions, such that no information exists on solute transport of potentially competitively adsorbing ions to the peat matrix. Additionally, recent studies suggest chloride (Cl^-) might not be conservative in peat, as assumed by many past peat solute transport studies. Based on measured and modelled adsorption isotherms, this study illustrates concentration dependent adsorption of Cl^- to peat occurred in equilibrium adsorption batch (EAB) experiments, which could be described with a Sips isotherm. However, Cl^- adsorption was insignificant for low concentrations (<500 mg L^{-1}) as used in breakthrough curve experiments (BTC). We found that competitive adsorption of Na^+, K^+, and NH_4^+ transport could be observed in EAB and BTC, depending on the dissolved ion species present. Na^+ followed a Langmuir isotherm, K^+ a linear isotherm within the tested concentration range (~10 – 1500 mg L^{-1}), while the results for NH_4^+ are inconclusive due to potential microbial degradation. Only Na^+ showed clear evidence of competitive behaviour, with an order of magnitude decrease in maximum adsorption capacity in the presence of NH_4^+ (0.22 to 0.02 mol kg^{-1}), which was confirmed by the BTC data where the Na^+ retardation coefficient differed between the experiments with different cations. Thus, solute mobility in peatlands is affected by competitive adsorption.

Keywords: reactive solute transport; anion adsorption; peat; breakthrough curve; nutrients; pH

1.0 Introduction

Large swaths of Canada's boreal, sub-arctic and arctic are dominated by organic soils, such as peat (Tarnocai et al., 2011), where increasing industrial development has enhanced the risk of contamination. Following controlled releases of contaminants, such as wastewater treatment wetlands, or accidental spills, a fundamental understanding of the processes governing solute transport is required to properly predict, mediate, and remediate contaminant plumes. However, critical knowledge gaps still remain in understanding solute transport in peat soils. For instance, only one field-scale study on reactive nutrient transport, such as sodium (Na^+), nitrate (NO_3^-), and ammonium (NH_4^+), exists (McCarter et al., 2017), and few laboratory-scale experiments (Kleimeier et al., 2014; Rezanezhad et al., 2012; Simhayov et al., 2018; Tiemeyer et al., 2017). The bulk of our understanding has been derived from studies on bog peat (Hoag and Price, 1997; Ours et al., 1997; Rosa and Larocque, 2008), degraded peat (Boudreau et al., 2009; Caron et al., 2015; Kleimeier et al., 2017; Liu et al., 2016; Rezanezhad et al., 2012; Tiemeyer et al., 2017), and more recently on undegraded fen peat (Kleimeier et al., 2017; Liu et al., 2017). These different peat soils can have different pore structures (Malmer et al., 2003) that cause both macropore and matrix flow (Weber et al., 2017b), potentially resulting in differing transport processes governing the movement of reactive solutes. Furthermore, monovalent cations, such as Na^+ or potassium (K^+), affect both the physical and geochemical conditions; potentially, resulting in changes to the transport and adsorption processes of other solutes. Sodium Chloride has been observed to both increase or decrease saturated hydraulic conductivity (K_{sat}), which has been attributed to pore dilation (Kettridge and Binley, 2010; Ours et al., 1997) or flocculation (Hoag and Price, 1997; Kettridge and Binley, 2010), respectively. These changes were attributed to changes in the ionic strength of the solution; thus, K^+ or other dissolved salts may have a similar effect. Furthermore, both Na^+ and K^+ can enhance the release of dissolved organic matter (Marschner and Kalbitz, 2003; Murphy et al., 1994), which potentially can mobilize bound contaminants (e.g., mercury) (Liao et al., 2009). The lack of clear understanding of the processes

governing the transport of multiple reactive solutes in peat leads to a large knowledge gap that needs to be filled as peat dominated landscapes come under increased development.

In many organic media transport studies, chloride (Cl^-), or other monovalent anions, have been used as a conservative tracer; yet, recently the conservative nature of Cl^- has been questioned (Caron et al., 2015). Indeed, Boudreau et al. (2009) observed bromide adsorption in both evaporation driven solute transport experiments and equilibrium adsorption batch experiments using peat-based organic horticultural potting media. However, Boudreau et al. (2009) assumed single porosity without investigating whether the peat-based organic potting media in fact reveals a single or dual porosity structure; yet, peat soils are commonly characterized as a dual (Rezanezhad et al., 2016) or even multi (Weber et al., 2017b) porosity substrate. Furthermore, at the field scale, both sodium chloride (Hoag and Price, 1995) and Na^+ (Ferlatte et al., 2015) have been used as tracers to determine physical or transport properties of peat and peatlands. Electrical conductivity (EC) has also been used as proxy measurement for Na^+ and Cl^- concentration (although it responds to all electrolytes in the solution) and may be misleading due to the reactivity of Na^+ and exchange with H^+ (Simhayov et al., 2018). From batch experiments on degraded fen peat, Rezanezhad et al. (2012) illustrated that Na^+ adsorption and desorption followed a reversible linear isotherm, and that equilibrium was established nearly instantaneously. However, in the presence of other cations, conservative (i.e., non-reactive) transport of Na^+ may occur, as assumed by Ferlatte et al. (2015), but this process has not been confirmed in peat or peatlands. Additionally, cations, such as Na^+ and K^+ (a common agricultural amendment along with nitrate or NH_4^+), may decrease the retardation of other cations through competitive adsorption processes, such as those identified for divalent metals (Ho and McKay, 1999; Ho et al., 2002). However, so far there has neither been a study on competitive adsorption of monovalent cations in peat soils, nor the subsequent effect on transport processes.

Peatlands are typically nutrient limited (Basiliko et al., 2006; Campbell and Bergeron, 2012; Wendel et al., 2011; Xing et al., 2011), resulting in low, if any concentrations of measurable NH_4^+. However,

with increasing development pressures, peatlands are more commonly being used as domestic wastewater treatment or polishing wetlands (Heikkinen et al., 1995; Kadlec, 2009; McCarter et al., 2017; Ronkanen and Klove, 2009); NH_4^+ can be a common constituent of domestic wastewater (Kadlec and Wallace, 2009). Unlike Na^+ and K^+, NH_4^+ is both geochemically and biologically reactive in peatlands and peat soils (Kadlec, 2009; McCarter et al., 2017; Ronkanen and Klove, 2009; Yates et al., 2012). Commonly, NH_4^+ is analysed as total nitrogen (NO_3^- and NH_4^+) (Kadlec, 2009; Ronkanen and Klove, 2009). Only McCarter et al. (2017) reported the transport rates and treatment efficiencies of NH_4^+ compared to other wastewater constituents, whereas both Kadlec (2009) and Ronkanen and Klove (2009) reported reaction rates and treatment efficiencies; not transport rates. In either case, under wastewater polishing conditions, peatlands readily remove NH_4^+ from the pore water through biogeochemical processes, likely ammonium oxidation followed by denitrification (Kleimeier et al., 2017; Rezanezhad et al., 2017) or anaerobic ammonium oxidation (Hu et al., 2011) depending on the redox conditions. Similar to Na^+ and K^+, NH_4^+ may affect the transport of other cations through competitive adsorption processes; however, there remains limited information on the transport of NH_4^+ in peat and the effect the presence of NH_4^+ has on the transport of other cations.

Understanding the interactions of dissolved cations with peat is critical to predicting solute transport in northern ecosystems under increasing developmental and agricultural pressures, in particular increasing nutrient inputs. However, much of the current work on reactive transport is based on chloride (Cl^-) or bromide (Br^-) as tracers, assuming these anions are not biogeochemically reactive and are truly conservative tracers. Recently this assumption has been questioned (Caron et al., 2015) but no conclusive evidence has been presented. Given the lack of knowledge on competitive adsorption of Na^+, K^+, and NH_4^+ and its potential effect on solute transport, and compounded with the possibility of Cl^- adsorption to peat, the objectives of this study are to 1) investigate the validity of the assumption that Cl^- may be considered as a conservative tracer in peat, 2) determine the effect multiple solutes (Na^+, K^+, and NH_4^+) have on equilibrium adsorption to peat, and 3) identify the effect of competitive adsorption on cation transport processes in peat.

2.0 Material and Methods

Peat samples were taken from a typical ladder fen in the James Bay Lowland (52°47'01 N, 83°53'12 W) near the DeBeers Victor Diamond Mine (McCarter et al., 2017; McCarter and Price, 2017a; McCarter and Price, 2017b). A sampling area of ~2 m^2 was identified in a low-lying preferential flow path, where ground vegetation was dominated by graminoid species and *Sphagnum* mosses and the water table was typically within 15 cm of the ground surface throughout the growing season (McCarter and Price, 2017a). The peat primarily consisted of light to moderately decomposed graminoid and *Sphagnum* species, with von Post (1926) decomposition levels between H2 and H4. In ladder fens, the highly non-linear transmissivity distribution within the peat results in the majority of water and solute movement to occur within the upper few centimetres of the ground surface (McCarter and Price, 2017a; McCarter and Price, 2017b). To capture the highly permeable upper peat layers, the upper 15 cm of peat was targeted for sampling. Large peat blocks ~20 x 20 x 20 cm were extracted by hand, and a cylindrical PVC pipe (10.2 cm i.d., 15 cm i.h) was used as a guide to carefully sub-section the peat block to the desired size, parallel to the direction of water flow. The samples (n=19 cores) were then individually wrapped in plastic wrap, while in the PVC pipe, and stored in a cooler for transport back to the University of Waterloo Wetlands Hydrology Laboratory for experimentation. Once at the Wetlands Hydrology Laboratory, the samples were further drained and frozen for sample preparation. The cores were randomly divided into 2 groups, the first group (3 cores) were used for equilibrium adsorption experiments, while the second group (16 cores) was chosen for the Breakthrough Curve (BTC) experiments. All experiments were performed at 20 ± 2 °C.

2.1 Equilibrium adsorption experiments

Group 1 peat (3 cores) was rinsed with Type II Ultra-Pure water and air dried until a low constant water content was reached (~0.2-0.3 cm^3 cm^{-3}). Roots or other woody debris were separated from the peat and the remaining peat material from each core was individually homogenised. Each of the homogenised cores represents one replicate; thus, for all equilibrium adsorption data three replicates exist. The peat from each core was then divided into 5 g samples (n=40 per core, n=120 total) and placed in sterile 50 mL polypropylene centrifuge tubes.

Equilibrium adsorption was determined for single (Na^+, K^+, NH_4^+, and Cl^-), dual-component (Na^+-K^+, Na^+- NH_4^+, and NH_4^+-K^+), and triple-component (Na^+-K^+- NH_4^+) mixtures at equal solution ionic strengths. None of the solutions were pH buffered to enable an assessment on the adsorption effect purely from the different cation compositions. The resulting pH of each solution was ~7 (Na^+ and K^+) and ~5.0 – 6.5 (NH_4^+). A total of five ionic strengths ($5.5x10^{-4}$, $2.8x10^{-3}$, $5.5x10^{-3}$, $2.8x10^{-2}$, and $5.5x10^{-2}$ mol L^{-1}) were chosen for each isotherm, and dissolved chloride salts used (i.e., NaCl, KCl, NH_4Cl; see Supplementary Information Table S1 for ion concentrations). Given the potential for biological turnover of NH_4^+, these isotherms were generated and are presented as Supplementary Information, only. The peat (5 g) was saturated with 20 mL of the target solution and the centrifuge tubes were capped. The centrifuge tubes were placed on a shaker table for 48 h at 40 RPM. To ensure at least 5 mL of extractant was available for analysis, the peat was manually squished and the liquid decanted into a 15 mL syringe. The decanted liquid was then filtered through a 0.45 µm PET filter and stored in a clean 15 mL polypropylene centrifuge tube at 4°C until IC analysis (DIONEX ICS 3000, IonPac AS18 and CS16 analytical columns) at the Biogeochemistry Laboratory at the University of Waterloo. Prior to IC analysis, the pH of each extractant was measured (Orion 9107BN pH/ATC Probe and Orion Star A324 pH/ISE Portable Multiparameter Meter). The resulting measured cation replicates were pooled and non-linear least-squared regression was used to fit models to describe linear, K^+, (Eq. 1) and non-linear, Na^+, (Langmuir, Eq. 2 & 4) adsorption isotherms and the best model was selected based on the root mean square error (R_{MSE}). Although competitive adsorption models do exist (Hinz, 2001; Limousin et al., 2007; Murali and Aylmore, 1983a; Murali and Aylmore, 1983b;

Murali and Aylmore, 1983c), there remain debates within the literature on the validity of these models (Allen and Brown, 1995; Ho and McKay, 1999; Limousin et al., 2007). However, averaged values for each concentration were used to generate the competitive Na^+ Langmuir isotherms to better compare the relative influence K^+ and NH_4^+ had on Na^+. Furthermore, deviations of the multi-component solution's maximum adsorption capacity (Q_{max}) from the single component solution can be used to infer whether competitive adsorption occurred and the relative influence of a given cation (Allen and Brown, 1995; Ho and McKay, 1999; Serrano et al., 2005). A Sips isotherm model, also known as a Langmuir-Freundlich isotherm (Sips, 1948), was fitted to the measured Cl^- data. Equations 1-3 relate the solid phase concentration (Q; mol kg^{-1}) to the aqueous phase concentrations (C; mol L^{-1}) through:

$$Q = K_d C \quad \text{Eq. (1)}$$

$$Q = Q_{max} \frac{L_i C}{1 + L_i C} \quad \text{Eq. (2)}$$

$$Q = Q_{max} \frac{a_s C^n}{1 + a_s C^n} \quad \text{Eq. (3)}$$

$$Q = Q_{max} \frac{L_i C}{1 + \sum_{j=1}^{q} L_j C_j} \quad \text{Eq. (4)}$$

where, K_d is the linear partitioning coefficient ($L^3\ M^{-1}$), L_i corresponds to the affinity of the i^{th} solute to sorb to the peat ($L^3\ M^{-1}$), Q_{max} is the maximum amount able to sorb onto the peat (mol M^{-1}), a_s is the Sips isotherm constant (-), n is the Sips non-linearity coefficient (-), L_j corresponds to the affinity of solute j in competition with solute i, and C_j is the aqueous concentration of j in competition with solute i. Adsorption isotherm fitting was performed in MATLab (MATLAB, 2017b) using the fitAdsorptionIsotherm code (Shimizu, 2014).

2.2 Breakthrough experiments

To prepare Group 2 for flow-through reactor (FTR) experiments, the ends of the frozen samples were cut (14.1 cm) to ensure any compression or smearing from the plastic wrap was removed and the cores were snugly inserted into acrylic pipe (10 cm i.d., 14.1 cm height) and left to thaw. The small decrease in dimensions from the sampling to the FTR cylinders, resulted in an extremely tight fit with no observable space between the peat and FTR cylinder wall. Once thawed, the cores were slowly saturated from the bottom and left for 48 hours. The end-caps of the FTRs were then placed on the submerged cores to ensure no air could enter the reactors. Each core was flushed with approximately three pore volumes of Type II Ultra-Pure water to ensure consistency of the pore water prior to experimentation. Changes in the ionic strength may result in pore dilation or pore clogging (Hoag and Price, 1997; Kettridge and Binley, 2010), which may change the hydrochemical transport within a core during a Breakthrough Curve (BTC) experiment. To mitigate this effect, each core was flushed with approximately 3 pore volumes of 500 mg L^{-1} Cl^- (NaCl; the upper-limit to be considered freshwater) followed by approximately six pore volumes of Type II Ultra-Pure water to ensure complete flushing of the NaCl. The hydraulic conductivity of each core was measured using a modified Darcy Permeameter under steady state conditions both before and during the NaCl flush to quantify any change in hydraulic parameters during the BTC experiments. The electrical conductivity of each core was measured prior to BTC experiments to ensure that no NaCl remained in the pore water prior to the beginning of the BTC experiments. For the solute BTC experiments, the cores were then randomly assigned into 4 different treatment groups (solutes: Na^+, K^+, NH_4^+, and Na^+ - K^+ - NH_4^+) with 4 replicates each.

The FTR was connected to two reservoirs, one containing Type II Ultra-Pure water and another the assigned tracer solution. Each BTC was generated using a peristaltic pump (WT600-3J, LongerPump, China) at a constant pumping rate of 0.12 mL s^{-1}. Initially, Type II Ultra-Pure water was injected into the core until a constant discharge of 0.12 mL s^{-1} was achieved. Tracer solutions of 500 mg L^{-1} Cl^- and the molecular equivalent of any of the cation combinations were prepared using chloride salts for each cation at pH ~6.5, the upper range of poor fens in the study region (McCarter et al., 2017). Once

constant discharge was achieved, the injection solution was instantaneously switched to the tracer solution and the time recorded as t_0. Every 15 minutes, a 50 mL sample (~ 5 % of total liquid sample volume) was collected and dissolved Cl^- measured using a Cl^- probe (Orion 9417B Cl^- ISE and Orion Star A324 pH/ISE Portable Multiparameter Meter) with a double junction reference electrode (Orion 900200 Ag/AgCl type) adjusted with an Ionic Strength Adjuster (Orion 940011). Every 30 minutes, a small 2 mL sample was decanted off the 50 mL sample for pH and cation analysis (see above). The electrical conductivity of the 50 mL sample was measured to provide an estimate of complete (both anion and cation) breakthrough. A dead-volume blank (Rajendran et al., 2008) was run and the resulting corrections were made to the data prior to inverse simulation to determine the solute transport parameters in the two region solute transport model (van Genuchten and Wagenet, 1989).

Once the BTC experiments were completed, the samples were drained to -100 mbar of pressure in a pressure cell (Soil Moisture Equipment Corp. model 1600) and weighed prior and after drainage to estimate the drainable porosity at -100 mbar (McCarter and Price, 2017b; Weber et al., 2017a). McCarter and Price (2017b) and Weber et al. (2017a) argue based on physical considerations to use this value in determining the active porosity of *Sphagnum* peat, allowing for an estimation of the effective porosity. The samples were then dried and the bulk density and porosity (assuming a particle density of 1.4, Redding and Devito (2006)) were determined.

2.3 Solute transport model

Assuming one dimensional steady state water flow in a homogeneous medium, the two-region (also mobile-immobile model; van Genuchten and Wagenet (1989)) is given in its dimensionless form as (Toride et al., 1993):

$$\beta R \frac{\partial c_m}{\partial T} = \frac{1}{P} \frac{\partial^2 c_m}{\partial Z^2} - \frac{\partial c_m}{\partial Z} - \omega(c_m - c_{im}) - \mu \quad \text{Eq. (4)}$$

$$(1-\beta) R \frac{\partial c_{im}}{\partial T} = \omega(c_m - c_{im}) - \mu \quad \text{Eq. (5)}$$

where c_m [-] and c_{im} [-] are the normalized solute concentration of the mobile and immobile phase, respectively, μ (T^{-1}) is a first order decay coefficient applied to the entire pore domain, dimensionless Z and T are space and time variables, P is the Peclet Number, and R, β, and ω are adjustable model parameters, which are given by the following well known equations (Toride et al., 1995),

$$P = v_m L / D_m \quad \text{Eq. (5a)}$$

$$T = v_m t / L \quad \text{Eq. (5b)}$$

$$Z = x / L \quad \text{Eq. (5c)}$$

$$\omega = \alpha L (\theta v_m) \quad \text{Eq. (5d)}$$

$$R = 1 + \rho_B K_d / \theta \quad \text{Eq. (5e)}$$

$$\beta = (\theta_m + f \rho_B K_d) / (\theta + \rho_B K_d) \quad \text{Eq. (5f)}$$

where, v_m [L T^{-1}] and D_m [L^2 T^{-1}] are average linear pore water velocity and the coefficient of dispersion of the mobile phase, respectively, α [T^{-1}] the first order rate coefficient of solute exchange between the mobile and immobile region, where f [-] is the fraction of sorption sites that equilibrate with the liquid mobile phase, ρ_B [M L^{-3}] is bulk density, and K_d [L^3 M] is the partitioning coefficient between the liquid and solid phase of linear solute sorption. For a non-sorbing solute with $K_d = 0$ the right-hand side of Eq. 5e reduces to 1 and that of Eq 5f to θ_m / θ, i.e. the fraction between the mobile and total water content, [-]. Column length L [L] (positive upward) is the length of the soil columns and an experimental set up dependent fixed parameter.

2.4 Parameterisation of the Mobile-Immobile solute transport model

The vector of unknown process model parameters, $\boldsymbol{x}$, was estimated by minimising the sum of square residuals by:

$$\Phi(\boldsymbol{x}) = \sum_{i}^{N} (C_i(t) - f_i(\boldsymbol{x}, t))^2 \quad (6)$$

where $\Phi(\boldsymbol{x})$ is the objective function value to be minimised, N the number of observations per breakthrough curve, C_i [-] the normalised measured concentration at time, t [T], and $f_i(\boldsymbol{x})$ [-] the corresponding normalised model predicted concentration. The mobile-immobile process model was calculated using CXTFIT (Toride et al., 1995) and global parameter estimation was done in R (R Development Core Team, 2018), using the differential evolution algorithm (Ardia et al., 2015; Mullen et al., 2011). This approach overcomes problems with estimating MIM parameters using local optimisers as reported by Rezanezhad et al. (2017).

Two cases were considered for the parameterisation, each with a different set of parameters to be estimated, one set for the investigated anion and one set for the cations. This differentiation was based on the expectation of a difference in adsorption behaviour. The first case looks at Cl^- breakthrough that was characterised without a term for adsorption, an assumption which is tested by accompanying experiments to determine the adsorption isotherm of Cl^-. For this reason, and due to the high number of parameters in the mobile-immobile solute transport model, two parameters, R and β were fixed *a priori* for the conservative tracer Cl^-. McCarter and Price (2017b) suggested that a pressure head of -100 cm could be used to delimit the proportion of mobile versus immobile pore space of ladder fen peat. Therefore, for each sample individually, the effective porosity, n_e [-] was determined as the fraction of the drainable porosity at a pressure head of -100 mbar to that of the total pore space, i.e. porosity. This was done by applying a constant pressure head of -100 cm in a pressure cell until no more water drained from the sample, which was determined by regularly taking the sample out of the pressure cell and weighing it. Since R = 1 under no adsorption scenario, we calculate β from knowledge of n_e by (Toride et al., 1995),

$$\beta = n_e/\phi \tag{7}$$

with ϕ as the total porosity determined from knowledge of the total sample volume, the oven dried mass and a solid particle density; Eq. 7 is therefore $\frac{\theta_m}{\theta}$. From fixing these, it follows that the remaining parameters were fitted ($\boldsymbol{x_1} = [v_m, D_e, \omega]$, Table 1). Additionally, the n_e (here described by the "active porosity", n_a) can be estimated from the resultant BTC analysis where,

$$n_a = Q_v/(v_m \cdot A) \tag{8}$$

and Q_v ($cm^3\ min^{-1}$) was the volumetric discharge and A (cm^2) was the surface area. Through calculating the n_e and n_a, a better understanding of the immobile pore space in peat can be elucidated.

In the second case, solute transport parameters were estimated to describe the observed breakthrough of the three monovalent cations (Na^+, K^+, $NH4^+$). Here, the parameters v_m and D_m were fixed to the previously, sample specific, estimated values based on the Cl^- breakthrough experiments. This was possible, since these parameters, per definition, are specific to the porous medium, therefore sample, and not solute specific. In the case of solute adsorption, β can no longer be estimated without knowledge of the adsorption coefficients K_d and f, which can be seen by inspection of Eq. 5f and was confirmed by Caron et al. (2015). For this reason we simultaneously estimate these parameters, and additionally ω, which is at least somewhat dependent on the solute specific molecular diffusion (Comegna et al. (2001); $\boldsymbol{x_2} = [R, \beta, \omega]$; Table 1).

To assess the goodness of fit, we calculated the root mean square error, R_{mse} [-] by

$$R_{mse} = \sqrt{\frac{1}{N}\sum_{i}^{N}(C_i(t) - f_i(\boldsymbol{x}, t))^2} \tag{9}$$

where, $C_i(t)$ is the measured normalised solute concentration at time t; $f_i(\boldsymbol{x}, t)$ is the model predicted value and N is the number of observations. The model parameter uncertainties (i.e. the approximation of the correlation matrix and the 95% confidence intervals) were calculated using the first-order second-moment method (Dettinger and Wilson, 1981).

Finally, we determined the sensitivity of the fixed parameters by a sensitivity index (Hamby, 1994), which numerically approximates the sensitivity of the parameters near the global optimum by using central differences to calculate the partial derives of the objective function with respect to the fixed parameters, $\boldsymbol{p_i}$;

$$\Phi_{sens,i} = \frac{\partial \Phi(\boldsymbol{p_i})}{\partial (p_i)} \left(\frac{p_i}{\Phi(\boldsymbol{x})}\right) \quad (10)$$

Eq. 10 assumes a linear dependence close to the minimum. However, this approach does not take possible correlations with the estimated parameters into account as they are not known; in that sense, $\Phi_{sens,i}$ is probably an overestimation of the true sensitivity and thus a conservative estimate.

3 Results

3.1 Hydro-physical peat properties

Bulk density varied between 0.05 – 0.10 g cm^{-3} with median bulk densities for each treatment group between 0.08 – 0.09 g cm^{-3} (Table 2), while porosity varied between 0.93 to 0.97 and median values for each treatment group between 0.94 – 0.95 (Table 2). The drainable porosity at -100 mbar (n_e) was on average 0.50 ± 0.07 (Table 2). Prior to flushing with 500 mg L^{-1} Cl^- (NaCl) the hydraulic conductivity varied between 2.1 – 14.9 m day^{-1} and increased during the NaCl flush (Table 2). All average (median) hydrophysical properties of each treatment group varied within 1 standard deviation of the mean (Table 2).

3.2 Equilibrium Adsorption Isotherms

A Langmuir (Na^+) or Linear (K^+) isotherm model was fit to the cation data, depending if they displayed non-linearity (Figure 1 & 2). Only Na^+ displayed competitive influences from either K^+ or NH_4^+, as illustrated by the decrease in Q_{max}, assuming that all exchange sites are available to each cation (Ho and McKay, 1999; Serrano et al., 2005). Therefore, any decrease in Q_{max} is due to the competitive cation filling the exchange sites at the expense of the target cation (Ho and McKay, 1999; Serrano et al., 2005). A slight increase in Q_{max} was observed when K^+ was present and a large decrease in Q_{max} was observed when NH_4^+ was present; regardless of other cations (Table 3). The presence of NH_4^+, regardless of other cations, resulted in a reduction in Q_{max} by an order of magnitude in both cases (Figure 1 and Table 3). This reduction in Na^+ Q_{max} was still prevalent and of a similar magnitude when excluding the largest concentrations from the single-component isotherms; thus, making the overall range tested similar between all isotherms (not shown). The competitive effects on Na^+ were further illustrated by fitting the average of each concentration to a competitive Langmuir isotherm, where both K^+ and NH_4^+ had higher affinity constants than Na^+, except for NH_4^+ when in solution with Na^+ and K^+ (Table S1). Conversely, K^+ fit well with both linear and Langmuir isotherms (Table 3) but no indications of non-linearity were observed in the data (Figure 2). Potassium K_d, regardless of solution composition, varied between 2.5 – 2.8 L kg^{-1}. Although NH_4^+ Langmuir and linear isotherms were generated (Figure S1), it is impossible to untangle the mixed effects of adsorption and microbial consumption observed in the BTC experiments. Chloride displayed weak adsorption to peat, resulting in highly non-linear "S" shaped (i.e., "S" class) isotherm (Hinz, 2001). Although other "S" class isotherms are available, convergence of the non-linear regression only occurred when using the Sips isotherm (Sips, 1948) (Figure 3). There was minimal adsorption at low concentrations but increased after ~0.005 mol L^{-1} (~160 mg L^{-1}), reaching a maximum of 0.05 mol kg^{-1} (Table 3). An approximate fit can be achieved using a linear isotherm (K_d = 0.78 L kg^{-1}, R_{MSE} = 2.9x10^{-2} mol kg^{-1}, Table 3). Both pH (adj. R^2 = 0.72, p-value < 0.0001) and calcium (adj. R^2 = 0.74, p-value <0.0001) were correlated with the total adsorbed cations, where pH decreased nearly exponentially, and calcium increased linearly as a greater abundance of cations were removed from the aqueous phase (Figure 4). Although all cation solutions followed the same general trends for both pH, NH_4^+ typically had lower pH than both Na^+ and K^+, but no statistical significance could be determined.

Similarly, all NH_4^+ solutions had a greater amount of aqueous phase calcium at the same adsorbed cation concentration (Figure 4). Although these deviations were not outside of the variability observed with Na^+ and K^+ (Figure 4), the slight deviation from Na^+ and K^+ could be linked to the applied unbuffered NH_4^+ solution which had lower pH's, since NH_4Cl is an acidic salt; in contrast NaCl and KCl that are neutral salts.

3.3 Breakthrough curve experiments

The MiM model was fit to each individual BTC, with or without adsorption depending on the ion of interest, and the median of the individually fit BTCs of each parameter was used to produce the median BTCs. The individual Cl^- BTCs could be described very well by the MiM model, with R_{MSE} values between $1.2x10^{-2}$ and $8.6x10^{-2}$ (Table 4). Moreover, the median modelled BTC showed good agreement with the observed data (Figure 5 & Table 4). Three BTCs (Na^+ 4, NH_4^+ 4, and Triple NH_4^+ 1) were discarded and not shown due to an inability to minimize the objective function (non-convergence of the measured data to the MiM model). Early breakthrough was observed in all cores, with an observed centre of Cl^- mass ($\frac{C}{C_0} = 0.5$) typically between 0.7 and 0.8 pore volumes due to the dual porosity structure of peat (Rezanezhad et al., 2017; Rezanezhad et al., 2012). Dispersivity values ranged from 2.8 – 24.6 cm, while the n_a (0.57 – 0.97, Table 4) was typically greater than the measured n_e value, which ranged from 0.42 – 0.67 (Table 2). Estimated dispersivity ($\lambda = D_m/v_m$) was on average 5.3 cm but two cores (K^+ 2 and Triple Mix 2) were well above 10 cm. Weak Cl^- adsorption as determined by the adsorption isotherms could be established (K_d = 0.78 L kg^{-1}), which results in an R of 1.07 (Eq. 5e) in the MiM model. This value is very small and cannot be considered significantly different to 1; thus, R was fixed to 1. Moreover, fixing it to 1.07 and fitting the remaining MiM parameters, did not lead to meaningful changes in the fitted parameters. However, we recognize that further extensive investigation of this phenomenon is required. The sensitivity indices of the fixed parameters were low with calculated median values of 0.3 for v_m, and 0.09 for β in the case of Cl^-, and overall cation experiments, the median values were 0.5 for v_m and 0.35 for D_m.

Using the resulting pore water velocities and dispersion variables determined from the Cl^- BTC fits, the cation transport parameters achieved good fits with the observed data (Table 5) and the median curves agreed well with the observed data (Table 5 & Figure 6 & 7). Similar to the equilibrium isotherms, the median R_{Na} decreased from a median of 1.98 to 1.01 between the single and multi-component solutions, suggesting competitive adsorption. Likewise, R_{NH4} decreased from 1.33 to 1.18 in the multicomponent solution; yet, remained near the values determined by the equilibrium batch experiments. The multi-component R_K typically remained within the maximum range (1.87 – 6.10) determined by the single component isotherm (1.54 – 4.60) and showed no evidence of competitive adsorption. In the NH_4^+ BTCs, a peak followed by a decrease and plateau in $C/C_{0\ NH4+}$ was observed, suggestive of biochemical degradation (Šimůnek and van Genuchten, 2008); thus, both adsorption and a first-order decay coefficient were simultaneously fit (Figure 7 & Table 5). The first-order degradation rate for NH_4^+ remained relatively constant between the single and competitive treatments (median $5.7x10^{-3}$ and $2.7x10^{-3}$ min^{-1}, respectively), where the difference is potentially due to differences in the input NH_4^+ concentration.

Notwithstanding the different starting pH of the NH_4^+ solutions, all cores and treatments pH and calcium followed the same general trends with the total aqueous phase cations, suggestive of some chemical non-equilibrium or dilution within the cores (Figure 8). However, there were no consistent correlations between solutions (not shown). The pH decreased slightly during most part of the experiment, followed by an increase towards the end, while calcium increased followed by a pronounced decrease. Overall, it appears pH follows an inverse trend to calcium. Over all cores pH varied between 5.9 and 6.5, while calcium concentrations were between 0.1 and 2.0 mol L^{-1}. Similar patterns of pH and calcium were observed with time (not shown), as the total aqueous phase cations were a proxy for time. In all cases, there was apparent chemical non-equilibrium with respect to pH and calcium, as both never reached a steady-state outflow by the end of the experiment, unlike the effluent cations.

4.0 Discussion

4.1 The conservative nature of chloride in peat

Recently, the conservative nature of Cl^- in organic soils and potting media has been questioned, yet there remained no empirical evidence of the potential reactive processes (Caron et al., 2015). The determined non-linear Cl^- adsorption isotherm in this study suggests possible weak adsorption of Cl^- in organic soils; however, given the low linear partitioning coefficient (0.78 L kg^{-1}) it did not measurably affect the fitting of the MiM model parameters within the concentration range tested. Given that no adsorption at low concentrations occurred, but adsorption increased with elevated aqueous phase concentration, an inhibiting process must be occurring at low aqueous phase concentrations. In most mineral soils, this isotherm shape suggests cooperative adsorption occurred or adsorption was inhibited by interactions with the organic material (Hinz, 2001; Ho et al., 2002). However, without further, and more extensive experimentation, the exact mechanism is unclear; yet, the relatively low Q_{max} of Cl^- (0.05 mol kg^{-1}) suggests a limited capacity to sorb onto peat. Notwithstanding the non-linear isotherm with little to no adsorption at low concentrations, at higher concentrations, Cl^- adsorption should be accounted for due to increased equilibrium adsorption (Hinz, 2001; Sips, 1948). Many studies of undisturbed and undecomposed peat have shown a distinct tailing in the BTC, similar to those observed in this study, which has been attributed to diffusion into the inactive porosity (physical non-equilibrium) (Hoag and Price, 1997; Kleimeier et al., 2017; Ours et al., 1997). Yet, this tailing could potentially be described by chemical adsorption rather than physical non-equilibrium (Simhayov et al., 2018). However, without a true conservative tracer to compare the Cl^- transport with, it is impossible to identify whether chemical or physical non-equilibrium or, more likely, a combination of both governs Cl^- transport in undisturbed and undecomposed peat. Although these findings do show Cl^- adsorption in this particular peat, they are exploratory in nature and require more detailed research to identify the broader applicability of Cl^- adsorption in peat. Chiefly, whether the "S" class (i.e., Sips or Freundlich isotherms) isotherm (Hinz, 2001; Limousin et al., 2007) describes a ubiquitous process in peat soils and what are the specific biogeochemical mechanism that govern Cl^-

adsorption are in peat. Additionally, it is unknown if Cl^- adsorption deviates from true conservative tracers (i.e., deuterated water or ^{18}O).

4.2 Physical transport properties of peat

Unlike the peat physical properties (bulk density, porosity, n_e, and K_{sat}), which showed minimal variability between replicates, a large variation in the shapes of the Cl^- BTCs could be observed. This resulted in a range of D_m values of approximately one order of magnitude (2.0 – 24.6 cm). Moreover, the large variations in n_a (0.57 – 0.95), ω (0.07 – 0.98), and λ (2.0 – 24.6 cm) suggest that the observed differences in BTCs can be attributed to the large variability in inter-pore connectivity and tortuosity between samples. Since this large variation could not be correlated to observable physical parameters; most importantly K_{sat} (6 – 23 cm day^{-1}), they do not serve as reliable predictors for solute transport. The centre of Cl^- mass was observed prior to one pore volume, suggesting the presence of interconnected macro-pores governing the majority of flow and transport, similar to studies in peat (Kleimeier et al., 2017; Rezanezhad et al., 2017). Concurrent to macropore flow, diffusion of Cl^- into the inactive porosity (as represented in its dimensionless form by ω) was variable and in some instances on the upper bounds set in the parameter estimation. The large values of ω indicates a near instantaneous equilibrium with the immobile phase; however, since there is a large range in ω values, no conclusive discussion can be made. It can be safely said, that under the given boundary conditions and flow rates, the proportion, connectivity, and flow path length of the mobile zone could be identified as the controlling factor on the solute transport, while the nature of the exchange rate between the mobile and immobile zone remains unclear.

In the MiM model, the effective or active porosity defined by β (Eq. 7) was fixed in this study to the measured drainable porosity at -100 mbar; resulting in an n_a that did not agree with the fixed β, as calculated with the n_e. This suggests there is a disconnect between the diffusion into the inactive

porosity, as governed by β, and the mobile fraction of the total porosity, as governed by the velocity. Contrary to previous solute transport studies in peat, the large calculated n_a suggest that most, if not all, of the porosity was hydraulically contributing to flow. In previous studies, n_a or n_e was typically 0.1 – 0.4 depending on the degree of decomposition and botanical composition (Hoag and Price, 1997; Kleimeier et al., 2014; Kleimeier et al., 2017; Rezanezhad et al., 2012; Rezanezhad et al., 2016). However, in some of these studies (Kleimeier et al., 2017; Rezanezhad et al., 2016), the average linear groundwater velocity was fixed to be proportional to the total porosity, rather than the n_e (or n_a); thus, as with this study, the calculated n_a does not agree with the estimated β. The results of the sensitivity analysis highlighted that in describing the presented data, the MiM model was more sensitive to change in average linear groundwater velocity than β. Given that it is prudent to fit the more sensitive parameter, fixing β value to a physically measured parameter, such as the drainable porosity at -100 mbar (McCarter and Price, 2017b; Weber et al., 2017b) will then lead to more accurate representation of the physical system. In either case, fixing a given parameter is not ideal but further research is required to determine the more efficient method for fitting BTC data or a more comprehensive solute transport model in peat, such as a dual-permeability transport model (Liu et al., 2017). These results do highlight the need for further research into the hydrophysical properties and processes governing solute transport in peat.

4.3 Equilibrium competitive adsorption

Regardless of the input solution pH, all equilibrium batch experiments pH decreased from between 5.5 to 4.8 at the lowest ionic strength to an asymptotic value of ~3.8 at the highest ionic strength and no single cation or mixture of cations displayed any deviation from this trend; suggestive that cation exchange with H^+ is an important exchange mechanism in peat. Furthermore, the asymptotic pH value observed (~3.8), at or near the lower pH limit observed in natural peatlands, which is~3.6 to 4.0 (Glaser et al., 2008; Mullen et al., 2000; Reeve et al., 1996; Ulanowski and Branfireun, 2013). In most acidic bog peatlands pH is thought to be a by-product of *Sphagnum* growth and decay through the

generation and release of organic acids (Abbott et al., 2013; Rudolph and Samland, 1985; van Breemen, 1995). However, these results potentially highlight a second mechanism of pH regulation in peatlands, where increases in aqueous cation concentration results in a decrease in pH due to ion exchange to the lower observed pH limit. Concurrently, the aqueous concentration of calcium increased, even though the peat was rinsed several times with Milli-Q water. When in the presence of NH_4^+, the rate of calcium release was greater (i.e., a larger slope between total adsorbed cations and calcium) but the total amounts released were similar, likely due to the asymptotic pH relationship driving ion exchange to calcium rather than H^+ or other weak organic acids, due to the lower starting pH of the NH_4^+ solutions. In either case, there appears to be a threshold release of H^+, as suggested by the large decrease in pH, required before other cations may be available for ion exchange in peat, which may have implications for mercury, or other pH dependent metals, dynamics in peatlands (Shotyk, 1988). The release of calcium and decrease in pH suggests that ion exchange was the primary adsorption mechanism within this poor fen peat.

In the equilibrium isotherms, Na^+ displayed non-linear adsorption to peat; resulting in a Langmuir isotherm. Previous studies in peat (Rezanezhad et al., 2012) suggest that Na^+ adsorption is linear; however, these studies were limited in their tested range (10 – 382 mg L^{-1}) and within this range, the Na^+ isotherms in this study were also linear. The deviation from linearity typically did not occur until much higher concentrations (> 1000 mg L^{-1}). The good fit with the Langmuir isotherm suggests that the true adsorption isotherm for peat is Langmuir with a very high Q_{max}, as could be expected from observations of large cation exchange capacities in various different peats (Kyzoil, 2002; Rippy and Nelson, 2007). Already within the concentration range tested by Rezanezhad et al. (2012), Na^+ exhibited non-linear adsorption behaviour when additional cations were present. This was also observable in the upper range of the multi-cation solution experiments. Given that non-linearity occurs at concentrations much higher than tested in the BTCs, it is reasonable to use a linear partitioning coefficient for Na^+, provided that the total concentration remains below a threshold of 1000 mg L^{-1}. Interestingly, Na^+ was the only cation influenced by the presence of other cations. The presence of

NH_4^+ (and NH_4^+ & K^+) created a much lower Q_{max} than just K^+ (approximately one order of magnitude, 0.22 to 0.02 L kg^{-1}); although both K^+ and NH_4^+ have similar adsorption affinities (Freeze and Cherry, 1979). The fitted competitive isotherm parameters generally support the Q_{max} analysis; however, the triple component solution results suggest that K^+ influenced the adsorption of Na^+ to a much greater extent than NH_4^+. Although these results may be due to variations in input pH (i.e., lower pH with higher NH_4^+ concentration), the lack of notable differences in the final pH indicates that although it may influence the relative amount of calcium released, it does not noticeably influence the ion exchange processes. It is noteworthy that at equal molarities Na^+ displayed a significant non-linearity, while K^+ did not; suggesting, that not all the adsorption sites on the peat were available to Na^+ (Allen and Brown, 1995; Ho and McKay, 1999). While the biogeochemical processes remain unclear, a possible explanation could be that the specific variation of organic molecules present in the peat are responsible for these observed results (Allen and Brown, 1995; Ho and McKay, 1999).

Contrary to Boudreau et al. (2009) who observed a Freundlich isotherm type K^+ adsorption in peat-based potting media when using maximum concentrations higher than those tested in this study (200 – 10,020 mg L^{-1}), K^+ adsorbed linearly to the peat, regardless of the concentration of other cations. Both of these results illustrate that, so far, no maximum K^+ adsorption has been observed in peat, highlighting its extremely large cation exchange capacity. In both the single-component and multi-component cases, K^+ showed a similar variation in replicated K_d suggesting the adsorption is insensitive to either the presence of Na^+ or NH_4^+. Although insensitivity to Na^+ was expected due to K^+ higher affinity for adsorption (Freeze and Cherry, 1979), the approximately equal adsorption affinity of NH_4^+ and K^+ would imply competition between the two cations unless adsorption sites were not limited. Since no competitive adsorption between K^+ and NH_4^+ was observed, it is unlikely that the adsorption sites were limited within the tested range. The abundant supply of adsorption sites agrees well with the high measured cation exchange capacity of peat in other studies (Kyzoil, 2002; Rippy and Nelson, 2007), suggesting that the observed decrease in Na^+ Q_{max} was due to competition rather than adsorption site limitation (Serrano et al., 2005). Regardless of the specific mechanism, the high

adsorption of K^+ in peat could limit the available K^+ for biological processes, independent of other cations, resulting in less of an observed effect on vegetation compared to other agricultural amendments (nitrogen or phosphorous), as found by Kirkham et al. (1996). Although Kirkham et al. (1996) found that phosphorous typically had a greater statistical effect than K^+, the study design was unable to specifically separate the effect of the individual amendments. Regardless, in most peatlands, even those used for agriculture, K^+ is typically not biologically limiting and not added as a regular agricultural amendment (Cuttle, 1983; Duren et al., 1997; El-Kahloun et al., 2003; Kirkham et al., 1996). Given the results of this study, the presence of dissolved or adsorbed K^+ will likely influence the transport of other cations through competitive adsorption, once the biogeochemical demand has been met.

4.4 Cation transport in peat

Retardation of Na^+ (R_{Na}), in a single cation injection solution (NaCl), in degraded and re-packed peat has been observed between 1.73 (Rezanezhad et al., 2012) and 3.07 (Simhayov et al., 2018), which agree with the observed values of this study (1.22 – 2.09). The resulting calculated Na^+ K_d values (Eq. 5e) (3.4 – 12.8 L kg^{-1}) were much larger than those determined from the batch experiments (2.8 L kg^{-1}), suggesting that equilibrium adsorption may not be the only occurring process during the solute transport experiments (Simhayov et al., 2018). This trend was further observed with K^+, illustrating systematic variations in K_d when determined from batch experiments and BTCs. Notwithstanding these results, unlike Simhayov et al. (2018), who found extremely poor fit using the convective dispersion equation and good fit using the non-linear adsorption kinetics one-site adsorption model, the good fit of the observed data to the simulation using equilibrium adsorption in the MiM model, suggests that Na^+ transport in peat could potentially be represented by either chemical or physical non-equilibrium depending on the choice of transport model. Nevertheless, both this study and Simhayov et al. (2018), among others (Hoag and Price, 1997; Kleimeier et al., 2017; Rezanezhad et al., 2017; Rezanezhad et al., 2012; Rezanezhad et al., 2016), rely on statistical fitting and numerical inverse

modelling to infer the governing processes and not direct observation, due to technological and physical limitations. Thus, there has yet to be direct observable evidence, only inferred evidence from BTC or batch experiments, of either physical or chemical non-equilibrium in peat; this remains a critical unanswered question in the literature.

The competitive adsorption effect of NH_4^+ on Na^+ adsorption was evident in the transport experiments, where a large decrease in R_{Na} (1.98 – 1.01) was observed under competitive conditions compared to the single cation condition, confirming the observed trends in the batch experiment results. Consequently, the $R_{Na} \sim 1$ suggests that no adsorption of Na^+ occurred and that Na^+ may be used a conservative tracer where other competitive cation concentrations are elevated, such as at the mineral peat interface (Ferlatte et al., 2015; Rosa and Larocque, 2008). The R_{NH4} slightly decreased under the competitive transport scenario (median R_{NH4} 1.33 to 1.18), suggesting some influence from either Na^+ or K^+; however, it is unclear which cation has the prominent effect, or if it is differences in pH that dominate the influence on NH_4^+. It is likely that K^+ was the primary cause of the reduced R_{NH4} value because Na^+ has lower adsorption affinity than K^+ and NH_4^+. However, due to confounding effects of microbial degradation on NH_4^+, further research is required to elucidate these processes. Unlike both NH_4^+ and Na^+, R_K did not decrease under competitive conditions but increased slightly; however, there are overlapping maximum and minimum R_K values between competitive and non-competitive conditions. Changes in the organic matter due to varied ionic strength (Ours et al., 1997) could potentially increase the adsorption due to increased surface area (Allen and Brown, 1995) or changes in available adsorption sites (Ho and McKay, 1999); there remains no evidence that the observed variation was simply not the true variation of K^+ adsorption in this particular peat. This suggests that the observed range in R_K and K_d reflects the intrinsic variability of K^+ adsorption in this particular peat and that the adsorption reactions were not rate limited. For agriculture on peat soils, the addition of K^+ and NH_4^+ may increase the mobility of NH_4^+ due to slight competitive adsorption; however, this effect would likely be limited due to biological uptake. Interestingly, there was a decrease in the diffusion into the inactive pores (i.e., lower median ω) in all cations under competitive conditions compared to

non-competitive conditions. Since this decrease affected all cations, and not only those affected by competitive adsorption processes, it is likely that this decrease was due to lower injected concentrations, thus mobile phase, rather than decreased adsorption in the inactive porosity. Although competitive adsorption has been identified with divalent cations (Ho and McKay, 1999), this is the first instance where it has been identified for mono-valent cations or confirmed to occur during solute transport in peat.

During the BTC experiments all combinations of influent solutions caused an initial decrease in pH and an increase in calcium concentration in the effluent, with the magnitude of change being sensitive to the ionic composition of the inflow. Partial recovery of pH and calcium concentration occurred later in the experiment. The single NH_4^+ and triple solution caused the largest decrease in pH and increase in calcium during the first half of the BTC and the largest recovery, likely due to the lower starting pH. The recovery period (i.e., the second half of the BTC), occurred in all cores when prolonged tailing of the influent cation was observed. Although the recovery of both pH and calcium was likely due to dilution of the pore water by the influent solution (pH ~6.5, 0.0 mol L^{-1} calcium), the lack of consistency in the magnitude of change and the co-varying relationship between pH and calcium makes it impossible to untangle whether pH, calcium, dilution, or another mechanism was governing this apparent non-equilibrium.

This apparent non-equilibrium, coupled with ion exchange, may increase the mobility of other metals such as mercury due to increased solubility at lower pH, and direct ion exchange processes that can increase the aqueous phase concentration (Melamed et al., 2000). In many northern peatlands, the mobility of mercury, specifically methylmercury, is of critical concern (McCarter et al., 2017; Schuster et al., 2018) due the high bioavailability and biomagnification of methylmercury (Hsu-Kim et al., 2018; Rudd, 1995). Historically, these annual low pH values typically coincide with summer-time low water tables (Glaser et al., 2008; Reeve et al., 1996; Ulanowski and Branfireun, 2013) and have been attributed to increased biological activity in the *Sphagnum* moss and decomposition processes

that generates organic acids through biochemical mechanisms (Abbott et al., 2013; Rudolph and Samland, 1985; van Breemen, 1995). During these low water table periods, the transmissivity of the peatland decreases exponentially, decreasing the pore water velocities by a similar magnitude, thus increasing the water and solute residence time (McCarter and Price, 2017a; Quinton et al., 2000), and lowering contaminant transport (McCarter and Price, 2017b). The increased water residence time extends the period (days instead of hours) over which pH equilibrium can occur, during which the release of H^+ ions likely contributes to the decrease in pH during the summer months. This hypothesis remains speculative, highlighting the need for further research on the mechanisms governing pH dynamics in peatlands. In any case, the release of H^+ from the peat matrix observed in both the equilibrium batch experiments and BTC experiments suggests that pH plays in important role in the mobility of dissolved and adsorbing cations within peat and peatlands.

4.5 Microbial Degradation of NH_4^+

Unlike in mineral soils, there remain few similar studies in peat on microbial-mediated degradation of NH_4^+ and its influence on solute transport (Kadlec, 2009; McCarter et al., 2017; Ronkanen and Klove, 2009). Within the wastewater treatment peatlands elevated NH_4^+ is commonly observed alongside elevated NO_3^-, and commonly described as total nitrogen (Kadlec, 2009; Ronkanen and Klove, 2009). It is the combination of anaerobic and aerobic biogeochemical/physical processes present in wastewater treatment peatlands results in near-complete immobilization and degradation of total nitrogen (Kadlec, 2009; Ronkanen and Klove, 2009); yet, transport rates and processes are rarely investigated (McCarter et al., 2017). Although the biochemical degradation of NH_4^+ was not the focus of this study, many of the modelled and measured NH_4^+ (i.e., NH_4^+ 1, NH_4^+ 3, Competitive NH_4^+ 3) BTCs showed decreases in C/C_0 in the long-plateaued tails in comparison to the other cations, suggesting biochemical degradation. In laboratory BTC experiments on un-degraded and degraded fen peat under anoxic conditions, Kleimeier et al. (2014) found average steady state nitrate removal rates of 0.056 µmol cm^{-3} hr^{-1}, much lower than this study's observed average steady state NH_4^+ removal

rates [(C_0-C_s) Q/V, where C_s is the stable steady state concentration of NH_4^+] of 8 – 17 µmol cm^{-3} hr^{-1}. Under anoxic conditions in peatlands, nitrate would be preferentially consumed (McCarter et al., 2017). However, the likely presence of oxygen in the tested cores, as the BTC water in this study was not de-oxygenated, suggests that aerobic microbial consumption was the primary removal pathway for NH_4^+. The presence of oxygen within the cores and likely aerobic microbial consumption initially preceded anoxic conditions, as reduced sulphur was detected through basic olfactory methods when flushing the cores after the BTC experiment. These changes in core oxygen status likely limits the extension of these results to the field scale, where it is assumed that anoxic conditions prevail (Bottrell et al., 2007; Rubol et al., 2012). However, under wastewater treatment conditions, dissolved oxygen present in wastewater effluent can raise the redox conditions and result in aerobic conditions and aerobic microbial consumption (Kadlec, 2009; Kadlec and Wallace, 2009). Regardless of the biochemical removal, there as a slight decrease in R_{NH4} under competitive conditions, suggesting complex interactions between the other dissolved cations and biochemical processes that influence the mobility of NH_4^+ in peat and peatlands.

5.0 Conclusions

In this study, the adsorption and transport processes of single and multiple solute mixtures were investigated using measured data from equilibrium adsorption batch experiments and breakthrough experiments. The observed data were used to calibrate different equilibrium adsorption isotherm models and the mobile-immobile solute transport model. The results from the equilibrium adsorption experiments showed that adsorption followed a non-linear Sips isotherm model for Cl^-, a Langmuir for Na^+, and linear for K^+. This clearly questions the *de facto* standard that Cl^- can be used as a conservative tracer in peat, at least at high concentrations. However, since Cl^- adsorbed negligibly at concentrations similar to those used in the breakthrough experiments, R was set to 1 for the parameterisation of the MiM model. While parameters could be generally well estimated using a global search algorithm, the parameter ω describing the diffusion into the inactive porosity remains

unclear due to high variability in the diffusion term. Here, we suggest experiments at lower flow velocities, such that the concentration difference in the flux averaged concentrations at the outlet of the breakthrough experiments can be detected against measurement error.

In the multiple cation adsorption experiments, Na^+ was clearly influenced by competitive adsorption behaviour, leading to lower adsorption in the presence of NH_4^+ but not K^+. Contrary to this, K^+ adsorption appeared uninfluenced by the presence of other ions. Microbial degradation precluded the analysis of the NH_4^+ equilibrium batch experiment data. However, the breakthrough experiments highlighted the potential for microbial degradation of NH_4^+ in peat and a slight decrease in adsorption when in the presence of other cations. Interestingly, there was an apparent lower limit of pH observed in the batch experiments that coincides with the lower observed pH values and low groundwater velocities in natural bogs and poor fens. This suggests that the low pH in these systems may be partly due to geochemical processes, in combination with the release of organic acids from *Sphagnum* mosses and decomposing peat. Although these were simple binary or trinary solutions, this study illustrates the need to account for these processes when studying solute transport in peat. It is evident that adsorption processes play a critical role in reactive solute transport in peat; particularly, the potential for anion adsorption questions the validity of previously determined peat transport parameters. However, there is still no conclusive evidence whether Cl^- adsorption is ubiquitous across different peat types and further investigation is warranted.

The following are the supplementary data related to this article.

Supplementary Fig S1

Supplementary Table S1: Competitive sodium Langmuir isotherms based on the average values for each triplicate concentration. Q_{max} was determined for the single component isotherm.

Supplementary Table S2: Input concentrations for the competitive equilibrium batch experiments.

Acknowledgements

The majority of data used are listed in the references, tables, and figures; all data is available upon request. The authors would like to acknowledge the NSERC Canadian Network for Aquatic Ecosystem Services (cnaes.ca) (NSERC NETGP417353-11) and NSERC Discovery 174626-2013-RGPIN for funding to JSP, and the De Beers Group of Companies (Victor Diamond Mine) for in-kind and logistical support. We would like to thank N. Toride and J. Šimůnek for providing details on the CXTFIT code. We would also like to thank Tasha-Leigh Gauthier, James Sherwood, and Katelyn Lutes for their help in the laboratory. Lastly, we are greatly appreciative of three anonymous reviewers and the editor who provided valuable insight and critiques on the manuscript.

References

Abbott, G.D., Swain, E.Y., Muhammad, A.B., Allton, K., Belyea, L.R., Laing, C.G. and Cowie, G.L., 2013. Effect of water-table fluctuations on the degradation of Sphagnum phenols in surficial peats. Geochimica et Cosmochimica Acta, 106: 177-191.https://doi.org/10.1016/j.gca.2012.12.013

Allen, S.J. and Brown, P.A., 1995. Isotherm analyses for single component and multi-component metal sorption onto lignite. Journal of Chemical Technology & Biotechnology, 62(1): 17-24.http://dx.doi.org/10.1002/jctb.280620103

Ardia, D., Mullen, K.M., Peterson, B.G. and Ulrich, J., 2015. 'DEoptim': Differential Evolution in 'R'.

Basiliko, N., Moore, T.R., Jeannotte, R. and Bubier, J.L., 2006. Nutrient Input and Carbon and Microbial Dynamics in an Ombrotrophic Bog. Geomicrobiology Journal, 23: 531-534.http://dx.doi.org/10.1080/01490450600897278

Bottrell, S.H., Mortimer, R.J.G., Spence, M., Krom, M.D., Clark, J.M. and Chapman, P.J., 2007. Insights into redox cycling of sulfur and iron in peatlands using high-resolution diffusive equilibrium thin film (DET) gel probe sampling. Chemical Geology, 244: 409-420.http://dx.doi.org/10.1016/j.chemgeo.2007.06.028

Boudreau, J., Caron, J., Elrick, D., Fortin, J. and Gallichand, J., 2009. Solute transport in sub-irrigated peat-based growing media. Canadian Journal of Soil Science, 89(3): 301-313.10.4141/cjss08023

Campbell, D. and Bergeron, J., 2012. Natural Revegetation of Winter Roads on Peatlands in the Hudson Bay Lowlands, Canada. Arctic, Antarctic, and Alpine Research, 44(2): 155-163.http://dx.doi.org/10.1657/1938-4246-44.2.155

Caron, J., Létourneau, G. and Fortin, J., 2015. Electrical conductivity breakthrough experiment and immobile water estimation in organic substrates: Is R = 1 a realistic assumption? Vadose Zone Journal, 14(9).10.2136/vzj2015.01.0014

Comegna, V., Coppola, A. and Sommella, A., 2001. Effectiveness of equilibrium and physical non-equilibrium approaches for interpreting solute transport through undisturbed soil columns. Journal of Contaminant Hydrology, 50(1): 121-138.https://doi.org/10.1016/S0169-7722(01)00100-0

Cuttle, S.P., 1983. Chemical properties of upland peats influencing the retention of phosphate and potassium ions. Journal of Soil Science, 34(1): 75-82.http://doi:10.1111/j.1365-2389.1983.tb00814.x

Dettinger, M.D. and Wilson, J.L., 1981. First order analysis of uncertainty in numerical models of groundwater flow part: 1. Mathematical development. Water Resources Research, 17(1): 149-161.http://dx.doi.org/10.1029/WR017i001p00149

Duren, I.C.V., Boeye, D. and Grootjans, A.P., 1997. Nutrient Limitations in an Extant and Drained Poor Fen: Implications for Restoration. Plant Ecology, 133(1): 91-100.10.2307/20050544

El-Kahloun, M., Boeye, D., Haesebroeck, V.V. and Verhagen, B., 2003. Differential Recovery of above- and Below-Ground Rich Fen Vegetation Following Fertilization. Journal of Vegetation Science, 14(3): 451-458.10.2307/3236523

Ferlatte, M., Quillet, A., Larocque, M., Cloutier, V., Pellerin, S. and Paniconi, C., 2015. Aquifer–peatland connectivity in southern Quebec (Canada). Hydrological Processes, 29(11): 2600-2612.http://dx.doi.org/10.1002/hyp.10390

Freeze, A. and Cherry, J., 1979. Goundwater. Prentice Hall, Inc, Upper Saddle River, NJ, USA.

Glaser, P.H., Wheeler, G., Gorham, E. and Wright, H., 2008. The Patterned Mires of the Red Lake Peatland , Northern Minnesota : Vegetation , Water Chemistry and Landforms. British Ecological Society 69: 575-599.

Hamby, D.M., 1994. A review of techniques for parameter sensitivity analysis of environmental models. Environmental Monitoring and Assessment, 32(2): 135-154.http://dx.doi.org/10.1007/bf00547132

Heikkinen, K., Ihme, R., Osma, A.-M. and Hartikainen, H., 1995. Phosphate Removal by Peat from Peat Mining Drainage Water during Overland Flow Wetland Treatment. Journal of Environmental Quality, 24(4): 597-602.http://dx.doi.org/10.2134/jeq1995.00472425002400040007x

Hinz, C., 2001. Description of sorption data with isotherm equations. Geoderma, 99(3–4): 225-243.http://dx.doi.org/10.1016/S0016-7061(00)00071-9

Ho, Y.S. and McKay, G., 1999. Competitive sorption of copper and nickel ions from aqueous solution using peat. Adsorption, 5(4): 409-417.http://dx.doi.org/10.1023/a:1008921002014

Ho, Y.S., Porter, J.F. and McKay, G., 2002. Equilibrium isotherm studies for the sorption of divalent metal ions onto peat: copper, nickel and lead single component systems. Water, Air, and Soil Pollution, 141(1): 1-33.http://dx.doi.org/10.1023/a:1021304828010

Hoag, R.S. and Price, J.S., 1995. A field-scale, natural gradient solute transport experiment in peat at a Newfoundland blanket bog. Journal of Hydrology, 172: 171-184.https://doi.org/10.1016/0022-1694(95)02696-M

Hoag, R.S. and Price, J.S., 1997. Effects of matrix diffusion on solute transport and retardation peat. Journal of Contaminant Hydrology, 28: 193-205.https://doi.org/10.1016/S0169-7722(96)00085-X

Hsu-Kim, H., Eckley, C.S., Achá, D., Feng, X., Gilmour, C.C., Jonsson, S. and Mitchell, C.P.J., 2018. Challenges and opportunities for managing aquatic mercury pollution in altered landscapes. Ambio, 47(2): 141-169.10.1007/s13280-017-1006-7

Hu, B.-I., Rush, D., van der Biezen, E., Zheng, P., van Mullekom, M., Schouten, S., Sinninghe Damste, J.S., Smoulders, A., Jetten, M.S.M. and Kartal, B., 2011. New Anaerobic, Ammonium-Oxidizing Community Enriched from Peat Soil. Applied and Environmental Microbiology, 77(3): 966-971.

Kadlec, R.H., 2009. Wastewater treatment at the Houghton Lake wetland: Hydrology and water quality. Ecological Engineering, 35: 1287–1311.http://dx.doi.org/10.1016/j.ecoleng.2008.10.001

Kadlec, R.H. and Wallace, S.D., 2009. Treatment Wetlands. CRC Press, Taylor & Francis Group, Boca Raton, FL.

Kettridge, N. and Binley, A., 2010. Evaluating the effect of using artificial pore water on the quality of laboratory hydraulic conductivity measurements of peat. Hydrological Processes, 24(18): 2629-2640.10.1002/hyp.7693

Kirkham, F.W., Mountford, J.O. and Wilkins, R.J., 1996. The Effects of Nitrogen, Potassium and Phosphorus Addition on the Vegetation of a Somerset Peat Moor Under Cutting Management. Journal of Applied Ecology, 33(5): 1013-1029.http://dx.doi.org/10.2307/2404682

Kleimeier, C., Karsten, U. and Lennartz, B., 2014. Suitability of degraded peat for constructed wetlands — Hydraulic properties and nutrient flushing. Geoderma, 228–229: 25-32.http://dx.doi.org/10.1016/j.geoderma.2013.12.026

Kleimeier, C., Rezanezhad, F., Van Cappellen, P. and Lennartz, B., 2017. Influence of pore structure on solute transport in degraded and undegraded fen peat soil. Mires and Peat, 19(18): 1-9.http://dx.doi.org/10.19189/MaP.2017.OMB.282

Kyzoil, J., 2002. Effect of Physical Properties and Cation Exchange Capacity on Sorption of Heavy Metals onto Peats. Polish Journal of Environmental Studies, 11(6): 713-718.

Liao, L., Selim, H.M. and DeLaune, R.D., 2009. Mercury Adsorption-Desorption and Transport in Soils. Journal of Environmental Quality, 38(4): 1608-1616.http://dx.doi.org/10.2134/jeq2008.0343

Limousin, G., Gaudet, J.P., Charlet, L., Szenknect, S., Barthès, V. and Krimissa, M., 2007. Sorption isotherms: A review on physical bases, modeling and measurement. Applied Geochemistry, 22(2): 249-275.https://doi.org/10.1016/j.apgeochem.2006.09.010

Liu, H., Forsmann, D.M., Kjærgaard, C., Saki, H. and Lennartz, B., 2017. Solute Transport Properties of Fen Peat Differing in Organic Matter Content. Journal of Environmental Quality.http://dx.doi.org/10.2134/jeq2017.01.0031

Liu, H., Janssen, M. and Lennartz, B., 2016. Changes in flow and transport patterns in fen peat following soil degradation. European Journal of Soil Science: n/a-n/a.10.1111/ejss.12380

Malmer, N., Albinsson, C., Svensson, B.M. and Walle, B., 2003. Interferences between Sphagnum and vascular plants : effects on plant community structure and peat formation. Oikos, 3: 469-482.

Marschner, B. and Kalbitz, K., 2003. Controls of bioavailability and biodegradability of dissolved organic matter in soils. Geoderma, 113(3): 211-235.https://doi.org/10.1016/S0016-7061(02)00362-2

MATLAB, 2017b. MATLAB and Statistics Toolbox Release. The MathWorks, Inc., Natick, Massachusetts, United States.

McCarter, C.P.R., Branfireun, B.A. and Price, J.S., 2017. Nutrient and mercury transport in a sub-arctic ladder fen peatland subjected to simulated wastewater discharges. Science of The Total Environment, 609(Supplement C): 1349-1360.https://doi.org/10.1016/j.scitotenv.2017.07.225

McCarter, C.P.R. and Price, J.S., 2017a. Experimental hydrological forcing to illustrate water flow processes of a subarctic ladder fen peatland. Hydrological Processes, http://dx.doi.org/10.1002/hyp.11127.DOI 10.1002/hyp.11127

McCarter, C.P.R. and Price, J.S., 2017b. The transport dynamics of chloride and sodium in a ladder fen during a continuous wastewater polishing experiment. Journal of Hydrology, 549: 558-570.http://dx.doi.org/10.1016/j.jhydrol.2017.04.033

Melamed, R., Trigueiro, F.E. and Villas Bôas, R.C., 2000. The effect of humic acid on mercury solubility and complexation. Applied Organometallic Chemistry, 14(9): 473-476.http://dx.doi.org/10.1002/1099-0739(200009)14:9<473::AID-AOC25>3.0.CO;2-W

Mullen, K.M., Ardia, D., Gil, D.L., Windover, D. and Cline, J., 2011. DEoptim: An R Package for Global Optimization by Differential Evolution. 2011, 40(6): 26.http://dx.doi.org/10.18637/jss.v040.i06

Mullen, S.F., Janssens, J.A. and Gorham, E., 2000. Acidity of and the concentrations of major and minor metals in the surface waters of bryophyte assemblages from 20 North American bogs and fens. Canadian Journal of Botany, 78: 718-727.

Murali, v. and Aylmore, L.A.G., 1983a. Competitive adsorption during solute transport in soils: 1. Mathematical models. Soil Science, 135(3): 143-150.

Murali, v. and Aylmore, l.A.G., 1983b. Competitive adsorption during solute transport in soils: 2. Simulations of competitive adsorption. Soil Science, 135(4): 203-213.

Murali, v. and Aylmore, l.A.G., 1983c. Competitive adsorption during solute transport in soils: 3. A review of experimental evidence of competitive adsorption and an evaluation of simple competition models. Soil Science, 136(5): 279-290.

Murphy, E.M., Zachara, J.M., Smith, S.C., Phillips, J.L. and Wietsma, T.W., 1994. Interaction of Hydrophobic Organic Compounds with Mineral-Bound Humic Substances. Environmental Science & Technology, 28(7): 1291-1299.http://dx.doi.org/10.1021/es00056a017

Ours, D., Siegel, D.I. and Glaser, P.H., 1997. Chemical dilation and the dual porosity of humified bog peat. Journal of Hydrology, 196: 348-360.http://doi.org/10.1016/S0022-1694(96)03247-7

Quinton, W.L., Gray, D.M. and Marsh, P., 2000. Subsurface drainage from hummock-covered hillslopes in the Arctic tundra. Journal of Hydrology, 237: 113-125.http://doi.org/10.1016/S0022-1694(00)00304-8

R Development Core Team, 2018. R: A language and environment for statistical computing. R Foundation for Statistitical Computing, Vienna, Austria.

Rajendran, A., Kariwala, V. and Farooq, S., 2008. Correction procedures for extra-column effects in dynamic column breakthrough experiments. Chemical Engineering Science, 63(10): 2696-2706.https://doi.org/10.1016/j.ces.2008.02.023

Redding, T.E. and Devito, K.J., 2006. Particle densities of wetland soils in northern Alberta, Canada. Canadian Journal of Soil Science, 86(1): 57-60.http://dx.doi.org/10.4141/S05-061

Reeve, A.S., Siegel, D.I. and Glaser, P.H., 1996. Geochemical controls on peatland pore water from the Hudson Bay Lowland: a multivariate statistical approach. Journal of Hydrology, 181(1–4): 285-304.http://dx.doi.org/10.1016/0022-1694(95)02900-1

Rezanezhad, F., Kleimeier, C., Milojevic, T., Liu, H., Weber, T.K.D., Van Cappellen, P. and Lennartz, B., 2017. The Role of Pore Structure on Nitrate Reduction in Peat Soil: A Physical Characterization of Pore Distribution and Solute Transport. Wetlands, 37(5): 951-960.http://dx.doi.org/10.1007/s13157-017-0930-4

Rezanezhad, F., Price, J.S. and Craig, J.R., 2012. The effects of dual porosity on transport and retardation in peat: A laboratory experiment. Canadian Journal of Soil Science, 92(5): 723-732.http://dx.doi.org/10.4141/cjss2011-050

Rezanezhad, F., Price, J.S., Quinton, W.L., Lennartz, B., Milojevic, T. and Van Cappellen, P., 2016. Structure of peat soils and implications for water storage, flow and solute transport: A review update for geochemists. Chemical Geology, 429: 75-84.http://dx.doi.org/10.1016/j.chemgeo.2016.03.010

Rippy, J.F.M. and Nelson, P.V., 2007. Cation Exchange Capacity and Base Saturation Variation among Alberta, Canada, Moss Peats. HortScience, 42(2): 349-352.

Ronkanen, A.-K. and Klove, B., 2009. Long-term phosphorus and nitrogen removal processes and preferential flow paths in Northern constructed peatlands. Ecological Engineering, 35.http://dx.doi.org/10.1016/j.ecoleng.2008.12.007

Rosa, E. and Larocque, M., 2008. Investigating peat hydrological properties using field and laboratory methods: application to the Lanoraie peatland complex (southern Quebec, Canada). Hydrological Processes, 22(12): 1866-1875.http://dx.doi.org/10.1002/hyp.6771

Rubol, S., Silver, W.L. and Bellin, A., 2012. Hydrologic control on redox and nitrogen dynamics in a peatland soil. Science of the Total Environment, 432: 37-46.http://dx.doi.org/10.1016/j.scitotenv.2012.05.073

Rudd, J., 1995. Sources of methyl mercury to freshwater ecosystems: A review. Water, Air, and Soil Pollution, 80(1-4): 697-713.10.1007/BF01189722

Rudolph, H. and Samland, J., 1985. Occurrence and metabolism of sphagnum acid in the cell walls of bryophytes. Phytochemistry, 24(4): 745-749.https://doi.org/10.1016/S0031-9422(00)84888-8

Schuster, P.F., Schaefer, K.M., Aiken, G.R., Antweiler, R.C., Dewild, J.F., Gryziec, J.D., Gusmeroli, A., Hugelius, G., Jafarov, E., Krabbenhoft, D.P., Liu, L., Herman-Mercer, N., Mu, C., Roth, D.A., Schaefer, T., Striegl, R.G., Wickland, K.P. and Zhang, T., 2018. Permafrost stores a globally significant amount of mercury. Geophysical Research Letters, 45.https://doi.org/10.1002/2017GL075571

Serrano, S., Garrido, F., Campbell, C.G. and García-González, M.T., 2005. Competitive sorption of cadmium and lead in acid soils of Central Spain. Geoderma, 124(1): 91-104.https://doi.org/10.1016/j.geoderma.2004.04.002

Shimizu, S., 2014. fitAdsorptionIsotherm, MATLab.

Shotyk, W., 1988. Review of the inorganic geochemistry of peats and peatland waters. Earth-Science Reviews, 25(2): 95-176.http://dx.doi.org/10.1016/0012-8252(88)90067-0

Simhayov, R.B., Weber, T.K.D. and Price, J.S., 2018. Saturated and unsaturated salt transport in peat from a constructed fen. SOIL, 4: 63-81.https://doi.org/10.5194/soil-4-63-2018

Šimůnek, J. and van Genuchten, M.T., 2008. Modeling Nonequilibrium Flow and Transport Processes Using HYDRUS. Vadose Zone Journal, 7(2): 782-797.10.2136/vzj2007.0074

Sips, R., 1948. On the Structure of a Catalyst Surface. The Journal of Chemical Physics, 16(5): 490-495.10.1063/1.1746922

Tarnocai, C., Kettles, I. and Lacelle, B., 2011. Peatlands of Canada. In: G.S.o. Canada (Editor). Natural Resources Canada.

Tiemeyer, B., Pfaffner, N., Frank, S., Kaiser, K. and Fiedler, S., 2017. Pore water velocity and ionic strength effects on DOC release from peat-sand mixtures: Results from laboratory and field experiments. Geoderma, 296(Supplement C): 86-97.https://doi.org/10.1016/j.geoderma.2017.02.024

Toride, N., Leij, F.J. and van Genuchten, M., 1995. The CXTFIT code for estimating transport parameters from laboratory or field tracer experiments. In: U.S.s. laboratory (Editor), research report no. 137. ARS, Riverside, CA, USDA.

Toride, N., Leij, F.J. and van Genuchten, M.T., 1993. A comprehensive set of analytical solutions for nonequilibrium solute transport with first-order decay and zero-order production. Water Resources Research, 29(7): 2167-2182.http://dx.doi.org/10.1029/93WR00496

Ulanowski, T.A. and Branfireun, B.A., 2013. Small-scale variability in peatland pore-water biogeochemistry, Hudson Bay Lowland, Canada. Science of the Total Environment, 454–455(0): 211-218.http://dx.doi.org/10.1016/j.scitotenv.2013.02.087

van Breemen, N., 1995. How Sphagnum bogs down other plants. Agriculture, 10.

van Genuchten, M.T. and Wagenet, R.J., 1989. Two-Site/Two-Region Models for Pesticide Transport and Degradation: Theoretical Development and Analytical Solutions. Soil Science Society of America Journal, 53(5): 1303-1310.http://dx.doi.org/10.2136/sssaj1989.03615995005300050001x

von Post, L., 1926. Södra Sveriges Torvtillgånger, I. Sver.Geo.Unders., C35(19 (2)).

Weber, T.K.D., Iden, S.C. and Durner, W., 2017a. A pore-size classification for peat bogs derived from unsaturated hydraulic properties. Hydrol. Earth Syst. Sci., 21(12): 6185-6200.http://dx.doi.org/10.5194/hess-21-6185-2017

Weber, T.K.D., Iden, S.C. and Durner, W., 2017b. Unsaturated hydraulic properties of *Sphagnum* moss and peat reveal trimodal pore-size distributions. Water Resources Research, 53(1): 415-434.http://dx.doi.org/10.1002/2016WR019707

Wendel, S., Moore, T.R., Bubier, J.L. and Blodau, C., 2011. Experimental nitrogen, phosphorus, and potassium deposition decreases summer soil temperatures, water contents, and soil CO_2 concentrations in a northern bog. Biogeosciences, 8: 585-595.http://dx.doi.org/10.5194/bg-8-585-2011

Xing, Y., Bubier, J.L., Moore, T.R., Murphy, M., Basiliko, N., Wendel, S. and Blodau, C., 2011. The fate of ^{15}N-nitrate in a northern peatland impacted by long term experimental nitrogen, phosphorus and potassium fertilization. Biogeochemistry, 103: 281-296.http://dx.doi.org/10.1007/s10533-010-9463-0

Yates, C.N., Wootton, B.C. and Murphy, S.D., 2012. Performance assessment of arctic tundra municipal wastewater treatment wetlands through an arctic summer. Ecological Engineering, 44(0): 160-173.http://dx.doi.org/10.1016/j.ecoleng.2012.04.011

Figure captions

Figure 1: Observed and fitted (Langmuir) Na+ adsorption isotherms under non-competitive and competitive scenarios. Note the log-log scale.

Figure 2: Observed and fitted (Linear) K+ adsorption isotherms under non-competitive and competitive scenarios. Note the log-log scale.

Figure 3: Observed and fitted Cl- sorption isotherm using a Sips isotherm (Sips, 1948; Hinz, 2001).

Figure 4: Aqueous pH and calcium in the extracted equilibrium batch experiment extracts regressed versus as a function of the total adsorbed cations.

Figure 5: Observed and fitted median Cl- BTCs. The fitted curve was derived by using the median value for each parameter determined by fitting each individual curve.

Figure 6: Median single component BTCs for each cation Na+ (top), K+ (middle), and NH4+ (bottom). The fitted curve was derived by using the median value for each parameter determined by fitting each individual curve, while the dashed line is the median curve for the chloride BTCs that match the cores used for each treatment. Note, Na+ 1 and NH4+ 4 are missing, since description with due to non-convergence of the inverse simulation of the MiM model was not possible.

Figure 7: Median competitive BTCs for each cation Na+ (top), K+ (middle), and NH4+ (bottom). The fitted curve was derived by using the median value for each parameter determined by fitting each individual curve, while the dashed line is the median curve for the chloride BTCs that match the cores

used for each treatment. Note, NH4+ 1 is missing due to non-convergence of the inverse simulation of the MiM model.

Figure 8: Observed pH and calcium concentration in the effluent of the BTC experiments for each applied BTC solution. The Total Aqueous Phase Cations represent a proxy for time, as the increase in Total Aqueous Phase Cations is directly related to the effluent concentrations and flow rate. Note, no apparent equilibrium was achieved for either pH or calcium, while equilibrium outflow was achieved for the individual cations.

Figure S1: Figure 1: Observed and fitted (Langmuir) NH4+ adsorption isotherms under non-competitive and competitive scenarios. Note the log-log scale.

Tables

Table 1: ANIONS: Fixed and estimated process model parameters, and lower and upper bounds for the estimated parameters, where the estimated pore water velocity v_m was bounded by two average linear groundwater velocities calculated from the measured flux density of the experiment (v_D; Darcy velocity) dividing by the determined porosity ϕ of the respective sample and an effective porosity of 5%, denoted by $\phi_{0.05}$. CATIONS: The estimated pore water velocity v_m and the dispersion coefficient D_m were fixed to the estimated parameter values for the anion breakthrough. Since β is dependent on R (eq. 2), and the cations are expected to show distinct adsorption, both parameters are estimated for the cation breakthrough curves. ω is dependent on molecular diffusion and has to be estimated for each ion individually. Explanation of the remaining process model parameters is given in the text.

		v_m	D_m	ω	R	β
		[cm min^{-1}]	[cm^2 min^{-1}]	[-]	[-]	[-]
ANION	*Lower bound*	v_D/ϕ	*1e-3*	*1e-1*	*Fixed to 1*	*NA, fixed*
ANION	*Upper bound*	$v_D/\phi_{0.05}$	*1e1*	*1e1*	*($K_d = 0$)*	*by eq. 2*
CATIONS	*Lower bound*	Fixed	Fixed	*1e-1*	*1*	*0*
CATIONS	*Upper bound*	Fixed	Fixed	*1e1*	*5*	1

Table 2: Hydrophysical properties of each BTC core separated by treatment. Hydraulic conductivity is separated into two runs. Pre-flush is prior to the NaCl flush, while mid-Flush is during the NaCl flush.

Core ID	Bulk Density	Porosity	n_e	K_{sat} (Pre-Flush)	K_{sat} (mid-Flush)
	[g cm^{-3}]	[-]	[-]	[cm day^{-1}]	[cm day^{-1}]
Sodium 1	0.07	0.95	0.50	7	14
Sodium 2	0.08	0.94	0.42	13	13
Sodium 3	0.09	0.94	0.51	11	22
Sodium 4	0.06	0.96	0.49	2	11
Potassium 2	0.08	0.95	0.51	12	14
Potassium 3	0.09	0.94	0.48	10	14
Potassium 4	0.10	0.94	0.44	4	6
Ammonium 1	0.08	0.93	0.45	15	21
Ammonium 3	0.10	0.95	0.67	15	23
Ammonium 4	0.05	0.97	0.61	8	18
Triple Mix 1	0.08	0.94	0.52	6	9
Triple Mix 2	0.07	0.95	0.59	11	22
Triple Mix 3	0.10	0.93	0.44	3	10
Triple Mix 4	0.09	0.93	0.43	6	14

Table 3: Sorption isotherm model coefficients. K_{ad} is the estimated partitioning coefficient determined from the Langmuir where $K_{ad} = Q_{max} L_i$ (Hinz, 2001; Limousin et al., 2007).

Ion	Additional Cation(s)	K_d [L kg^{-1}]	K_{ad} [L kg^{-1}]	Q_{max} [mol kg^{-1}]	L_i (a_s) [L kg^{-1} (-)]	n [-]	Linear R_{MSE} [mol kg^{-1}]	R_{MSE} [mol kg^{-1}]
Sodium	-	1.9	2.81	0.22	12.64	-	5.1E-03	3.3E-03
Sodium	Potassium	2.4	3.6	0.25	14.5	-	2.0E-03	4.2E-03
Sodium	Ammonium	2.6	4.3	0.04	98	-	2.0E-03	6.6E-04
Sodium	Potassium & Ammonium	2.1	4.1	0.02	192	-	1.1E-03	5.6E-04
Potassium	-	2.6	-	-	-	-	3.4E-03	-
Potassium	Sodium	2.8	-	-	-	-	2.0E-03	-
Potassium	Ammonium	2.7	-	-	-	-	1.8E-03	-
Potassium	Sodium & Ammonium	2.5	-	-	-	-	1.3E-03	-
Ammonium	-	1.5	1.7	0.20	8	-	2.8E-03	2.8E-03
Ammonium	Sodium	1.7	2.1	0.03	84	-	1.4E-03	1.8E-03
Ammonium	Potassium	1.3	2.0	0.02	96	-	1.3E-03	1.4E-03
Ammonium	Sodium & Potassium	1.0	1.7	0.01	139	-	1.4E-04	4.6E-04
Chloride	-	0.78	-	0.05	817	0.53	2.9E-02	4.1E-03

Table 4: Conservative solute transport parameters derived from the Cl^- BTCs. Dispersivity (α_m) was estimated by D_m/v_m. The v_m and D_m were used to estimate the reactive cation transport parameters (Table 5). The median values are the average parameters determined from replicates, while the median chloride is the average values for all 13 cores.

	v_m	D_m	β	ω	λ	n_a	R_{MSE}	R^2
	[cm min^{-1}]	[cm^2 min^{-1}]	[-]	[-]	[cm]	[-]	[-]	
Sodium 1	0.15	0.95	0.53	0.16	6.3	0.57	2.2E-02	0.99
Sodium 2	0.15	0.71	0.45	9.98	4.8	0.61	5.2E-02	0.96
Sodium 4	0.11	0.37	0.51	0.27	3.4	0.80	3.5E-02	0.99
Potassium 2	0.10	2.37	0.54	0.04	24.6	0.95	2.4E-02	0.96
Potassium 3	0.15	1.03	0.51	8.26	7.1	0.61	2.6E-02	0.96
Potassium 4	0.10	0.54	0.47	8.38	5.3	0.90	4.3E-02	0.97
Ammonium 1	0.10	0.28	0.48	0.31	2.8	0.87	2.5E-02	0.99
Ammonium 3	0.09	0.57	0.70	0.07	6.0	0.97	1.2E-02	1.00
Ammonium 4	0.10	0.30	0.64	0.18	3.2	0.94	3.6E-02	0.98
Triple Mix 1	0.12	0.91	0.55	9.50	7.5	0.75	2.2E-02	0.98
Triple Mix 2	0.15	1.97	0.62	0.10	13.2	0.64	1.4E-02	1.00
Triple Mix 3	0.13	0.40	0.47	1.51	3.20	0.72	2.5E-02	0.99
Triple Mix 4	0.10	0.20	0.46	9.75	2.0	0.89	8.6E-02	0.92
Median Sodium	0.15	0.71	0.45	0.53	4.8	0.61	-	-
Median Potassium	0.10	1.03	0.51	8.26	7.1	0.90	-	-
Median Ammonium	0.10	0.30	0.64	0.18	3.2	0.94	-	-
Median Triple Mix	0.12	0.66	0.51	5.51	5.3	0.74	-	-
Median Chloride	0.11	0.57	0.51	0.64	5.3	0.80	1.7E-01	0.63

Table 5: Reactive cation transport parameters determined from fitting the observed data to the MiM model. The v_m and D_m were estimated from the Cl^- BTCs (Table 4). The median values are the average parameters determined from replicates.

	v_m	D_m	R	β	ω	μ	R_{MSE}	R^2
	[cm min^{-1}]	[cm^2 min^{-1}]	[-]	[-]	[-]	[min^{-1}]	[-]	
Sodium 1	0.15	0.95	1.98	0.56	0.03	-	3.8E-02	0.97
Sodium 2	0.15	0.71	2.09	0.42	0.05	-	5.9E-03	1.00
Sodium 4	0.11	0.37	1.22	0.01	0.08	-	1.8E-02	0.92
Potassium 2	0.10	2.37	4.60	0.30	0.03	-	1.8E-02	0.98
Potassium 3	0.15	1.03	2.30	0.28	0.13	-	1.9E-02	0.98
Potassium 4	0.10	0.54	2.47	0.59	0.10	-	1.2E-02	1.00
Ammonium 1	0.10	0.28	1.54	0.04	0.74	5.7E-03	2.4E-02	0.99
Ammonium 3	0.09	0.57	1.25	0.32	0.49	7.0E-04	1.6E-02	0.99
Ammonium 4	0.10	0.30	1.33	0.04	3.82	1.1E-02	4.3E-02	0.97
TRP Sodium 1	0.12	0.91	1.00	0.64	0.02	-	2.4E-02	0.97
TRP Sodium 2	0.15	1.97	1.00	0.48	0.03	-	4.6E-02	0.94
TRP Sodium 3	0.13	0.40	1.02	0.64	0.01	-	2.6E-02	0.98
TRP Sodium 4	0.10	0.20	1.01	0.57	0.01	-	4.4E-02	0.95
TRP Potassium 1	0.12	0.91	6.10	0.27	0.04	-	1.2E-02	0.99
TRP Potassium 2	0.15	1.97	1.87	0.50	0.05	-	2.3E-02	0.99
TRP Potassium 3	0.13	0.40	5.18	0.31	0.04	-	1.6E-02	0.99
TRP Potassium 4	0.10	0.20	2.49	0.46	0.03	-	3.5E-02	0.98
TRP Ammonium 2	0.15	1.97	1.17	0.56	0.12	2.7E-03	2.1E-02	0.99
TRP Ammonium 3	0.13	0.40	1.46	0.65	0.22	9.6E-04	2.0E-02	0.99
TRP Ammonium 4	0.10	0.20	1.18	0.71	0.23	6.8E-03	2.6E-02	0.99
Median Sodium	0.15	0.71	1.98	0.42	0.05	-	4.6E-02	0.96
Median Potassium	0.10	1.03	2.47	0.30	0.10	-	1.1E-01	0.79
Median Ammonium	0.10	0.30	1.33	0.04	0.74	5.7E-03	1.5E-01	0.73
Median TRP Sodium	0.12	0.66	1.01	0.60	0.01	-	8.2E-02	0.94
Median TRP Potassium	0.12	0.66	3.84	0.38	0.04	-	6.3E-02	0.92
Median TRP Ammonium	0.13	0.40	1.18	0.65	0.22	2.7E-03	3.6E-02	0.98

Highlights

1. Observed concentration dependent chloride adsorption to peat for solutions > 500 mg/L.
2. Competitive adsorption and transport observed between sodium, potassium, and ammonium in peat.
3. Under competitive conditions, sodium transport behaved conservatively.
4. Lower limit of pH observed coincides with lower limit of reported bog pH values

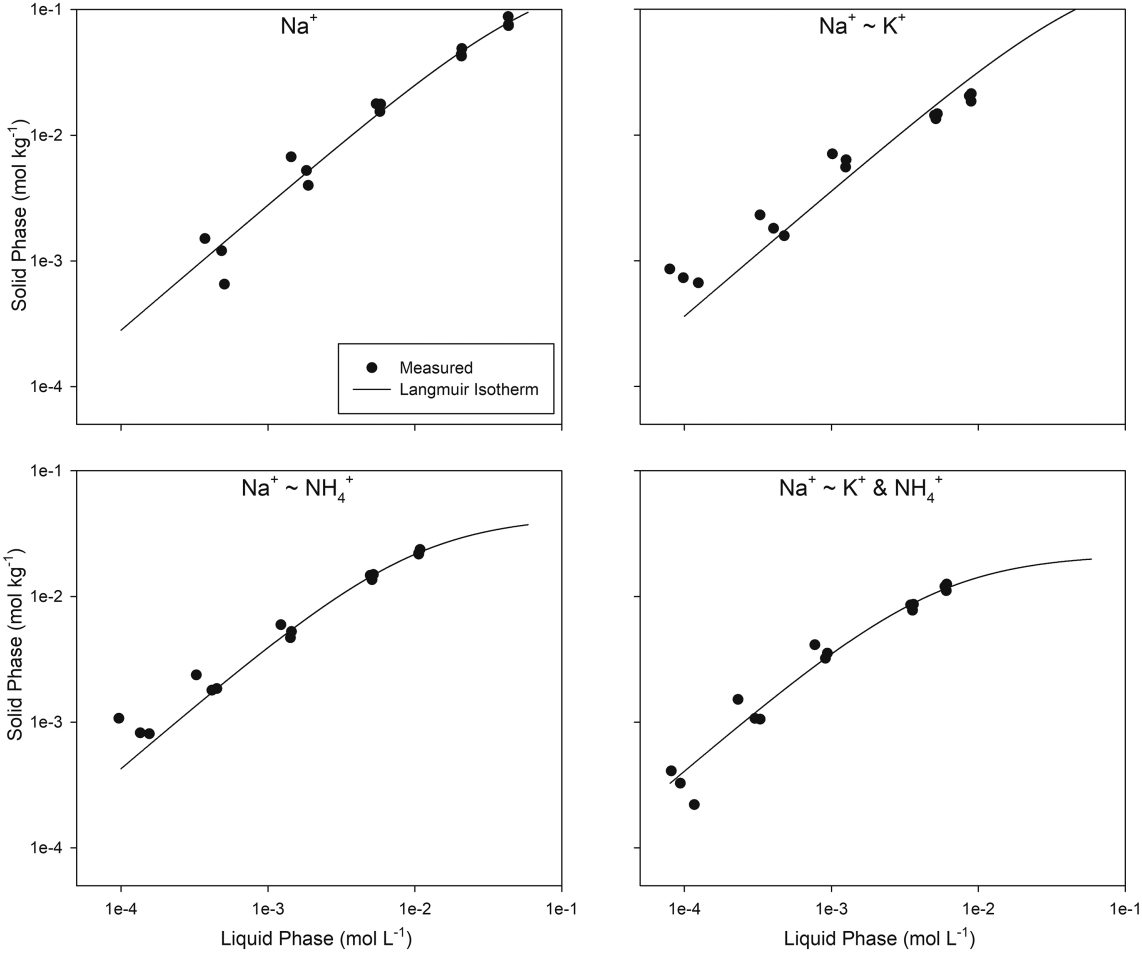
Na+
Na+ ~ K+
Na+ ~ NH4+
Na+ ~ K+ & NH4+
Measured
Langmuir Isotherm
Solid Phase (mol kg-1)
Liquid Phase (mol L-1)
1e-1
1e-2
1e-3
1e-4

Figure 1

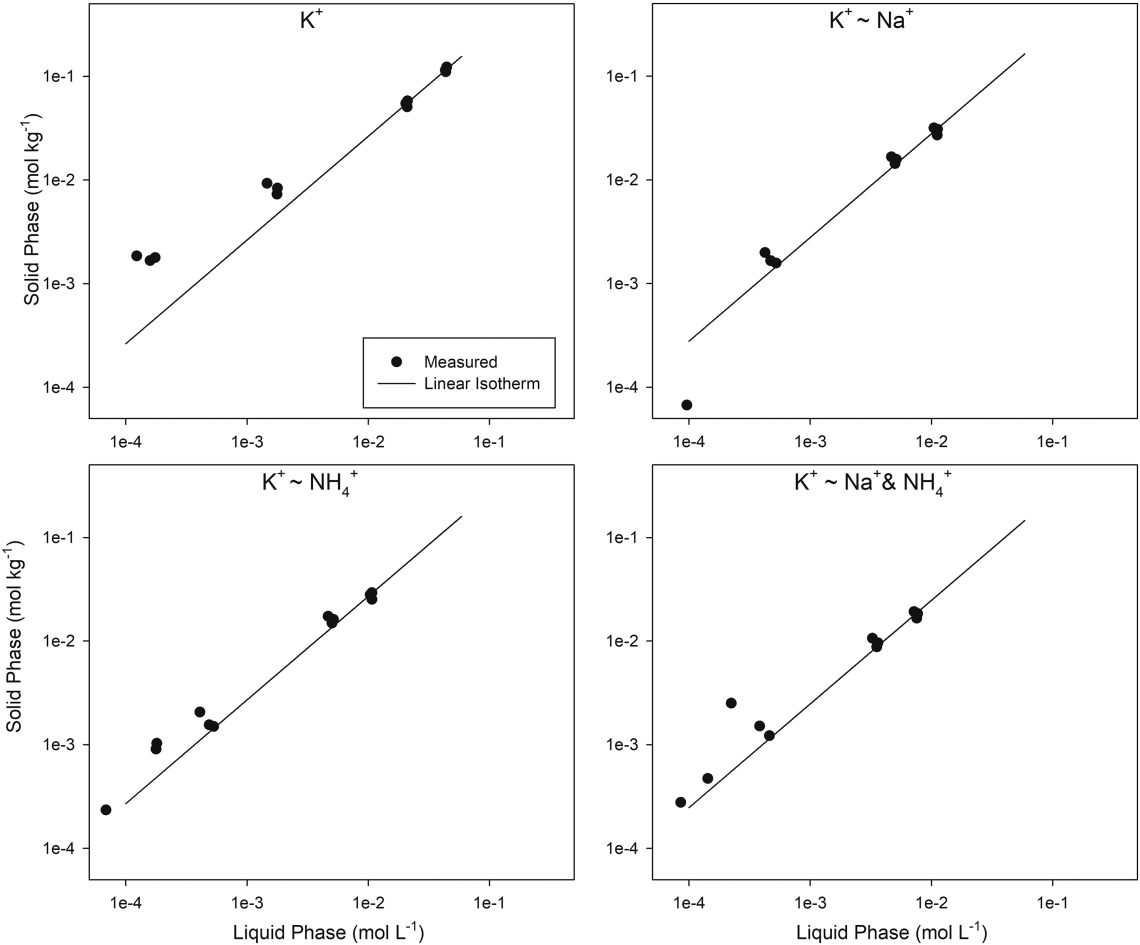
K+
K+ ~ Na+
K+ ~ NH4+
K+ ~ Na+& NH4+
Solid Phase (mol kg-1)
Liquid Phase (mol L-1)
1e-1
1e-2
1e-3
1e-4
Measured
Linear Isotherm

Figure 2

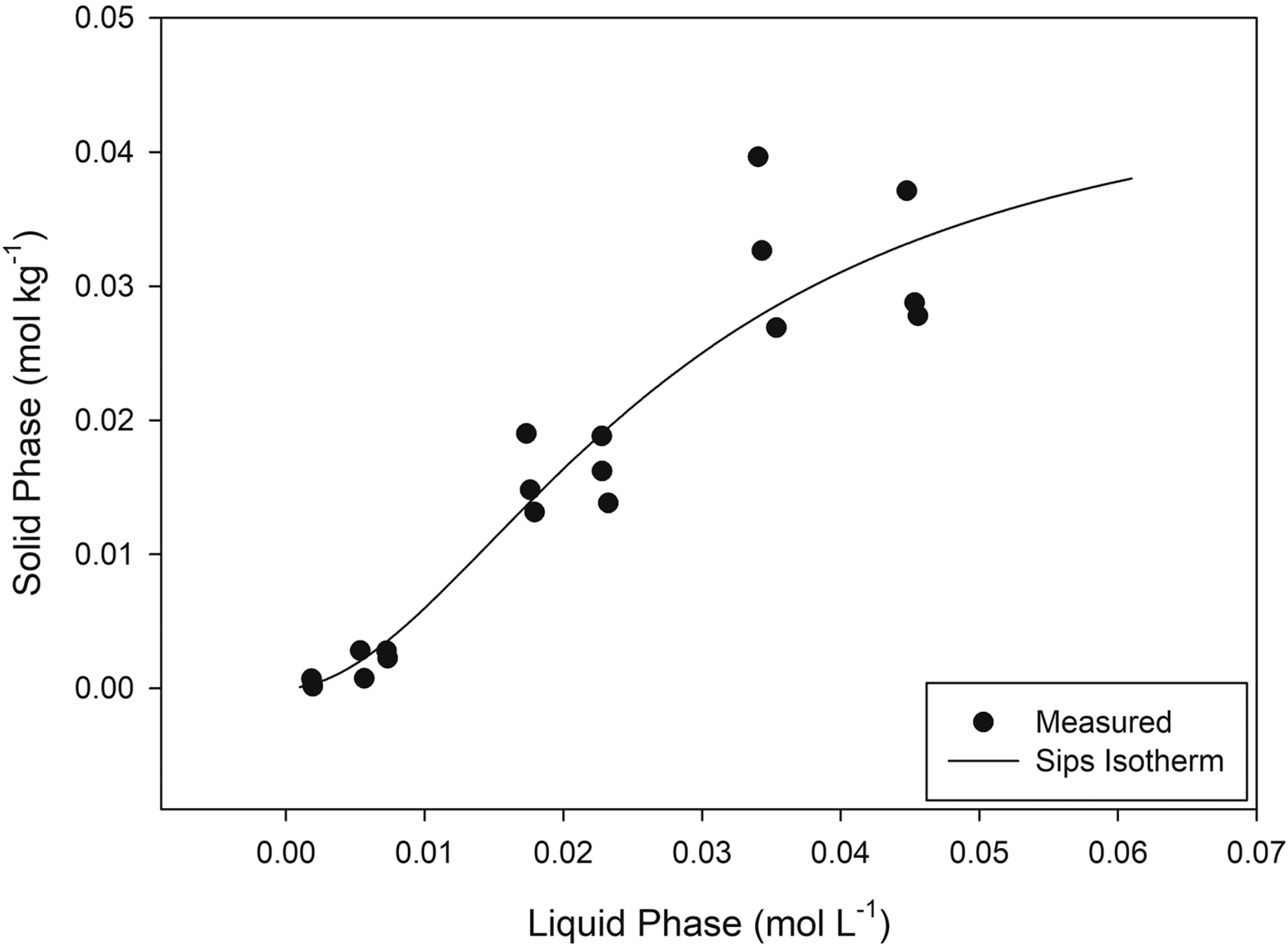
0.05
0.04
0.03
0.02
0.01
0.00
Solid Phase (mol kg-1)
0.00
0.01
0.02
0.03
0.04
0.05
0.06
0.07
Liquid Phase (mol L-1)
Measured
Sips Isotherm

Figure 3

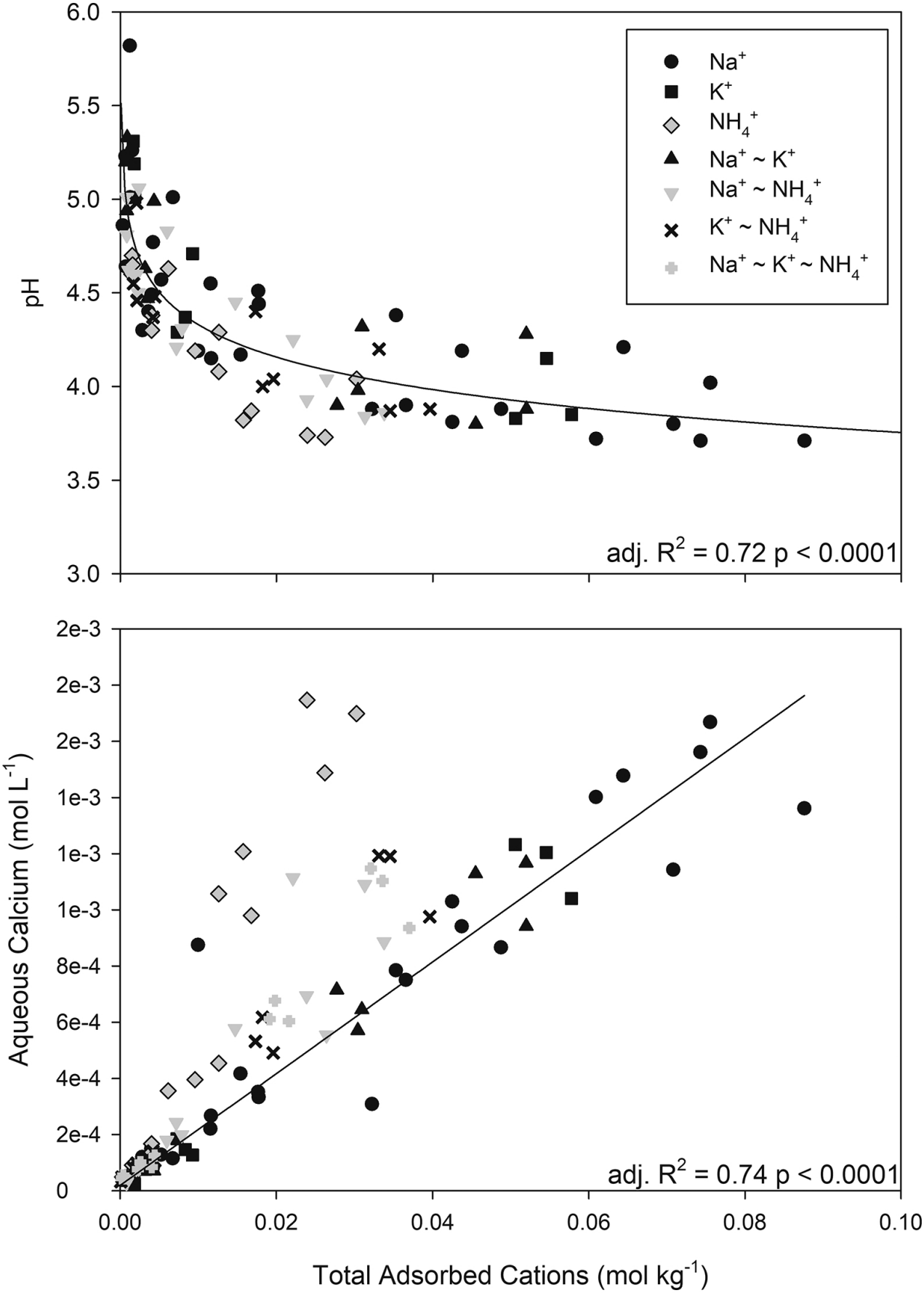
6.0
5.5
5.0
4.5
4.0
3.5
3.0
pH
Na+
K+
NH4+
Na+ ~ K+
Na+ ~ NH4+
K+ ~ NH4+
Na+ ~ K+ ~ NH4+
adj. R2 = 0.72 p < 0.0001
2e-3
2e-3
2e-3
1e-3
1e-3
1e-3
8e-4
6e-4
4e-4
2e-4
0
Aqueous Calcium (mol L-1)
adj. R2 = 0.74 p < 0.0001
0.00
0.02
0.04
0.06
0.08
0.10
Total Adsorbed Cations (mol kg-1)

Figure 4

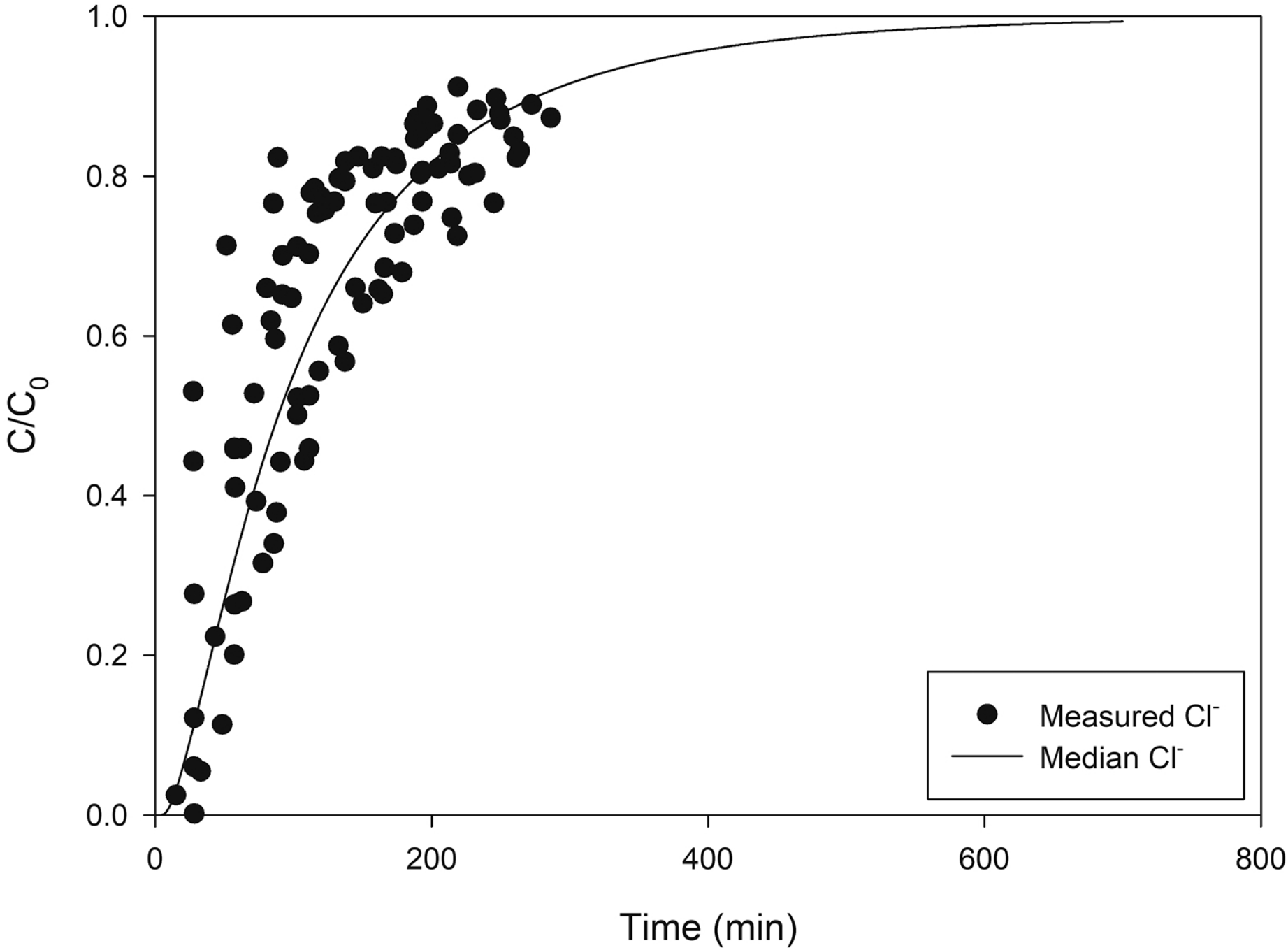
1.0
0.8
0.6
0.4
0.2
0.0
C/C0
0
200
400
600
800
Time (min)
Measured Cl-
Median Cl-

Figure 5

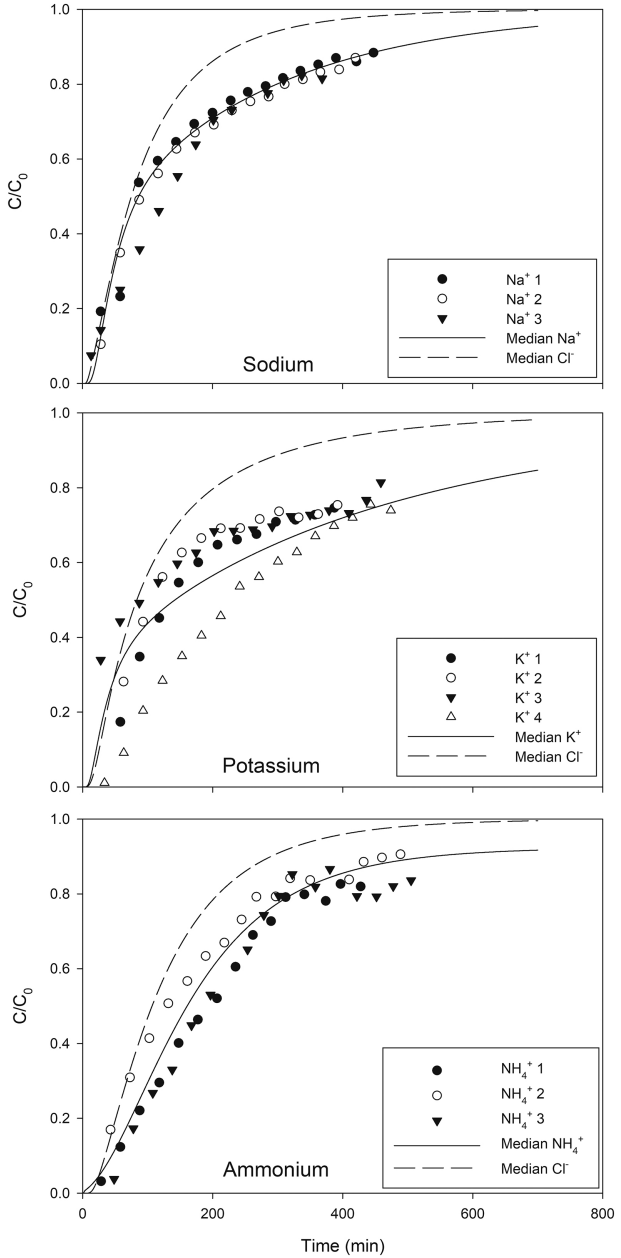
C/C0
Sodium
Na+ 1
Na+ 2
Na+ 3
Median Na+
Median Cl-
Potassium
K+ 1
K+ 2
K+ 3
K+ 4
Median K+
Median Cl-
Ammonium
NH4+ 1
NH4+ 2
NH4+ 3
Median NH4+
Median Cl-
0.0
0.2
0.4
0.6
0.8
1.0
0
200
400
600
800
Time (min)

Figure 6

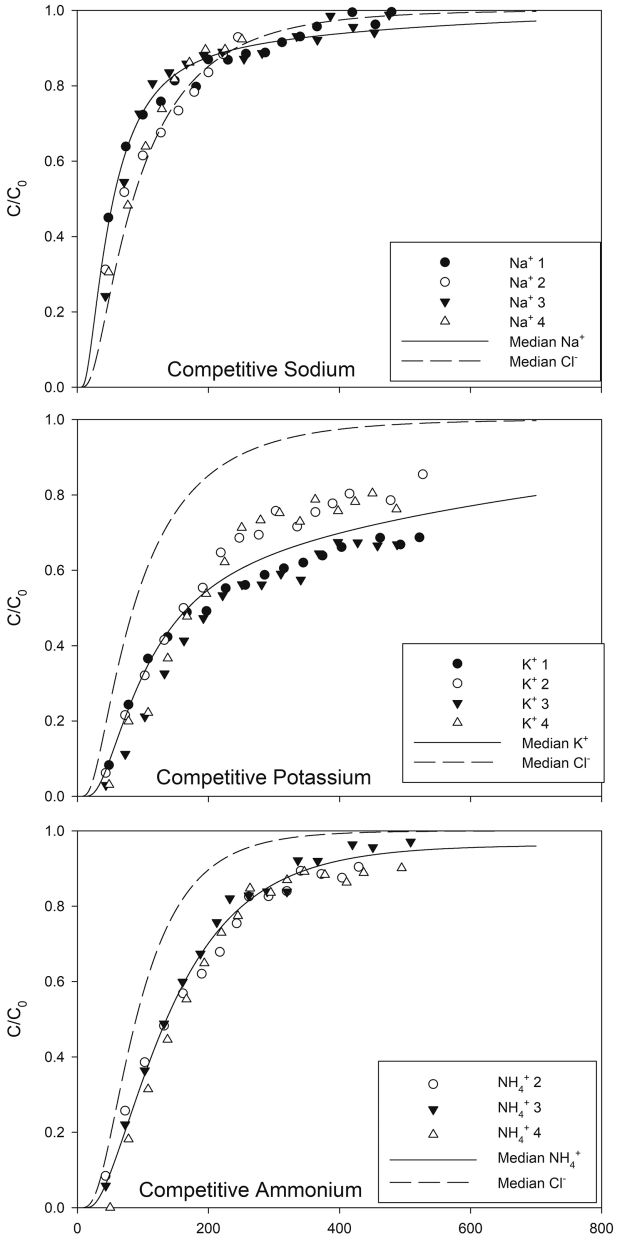
C/C0
Competitive Sodium
Na+ 1
Na+ 2
Na+ 3
Na+ 4
Median Na+
Median Cl-
Competitive Potassium
K+ 1
K+ 2
K+ 3
K+ 4
Median K+
Median Cl-
Competitive Ammonium
NH4+ 2
NH4+ 3
NH4+ 4
Median NH4+
Median Cl-
0
200
400
600
800
Time (min)

Figure 7

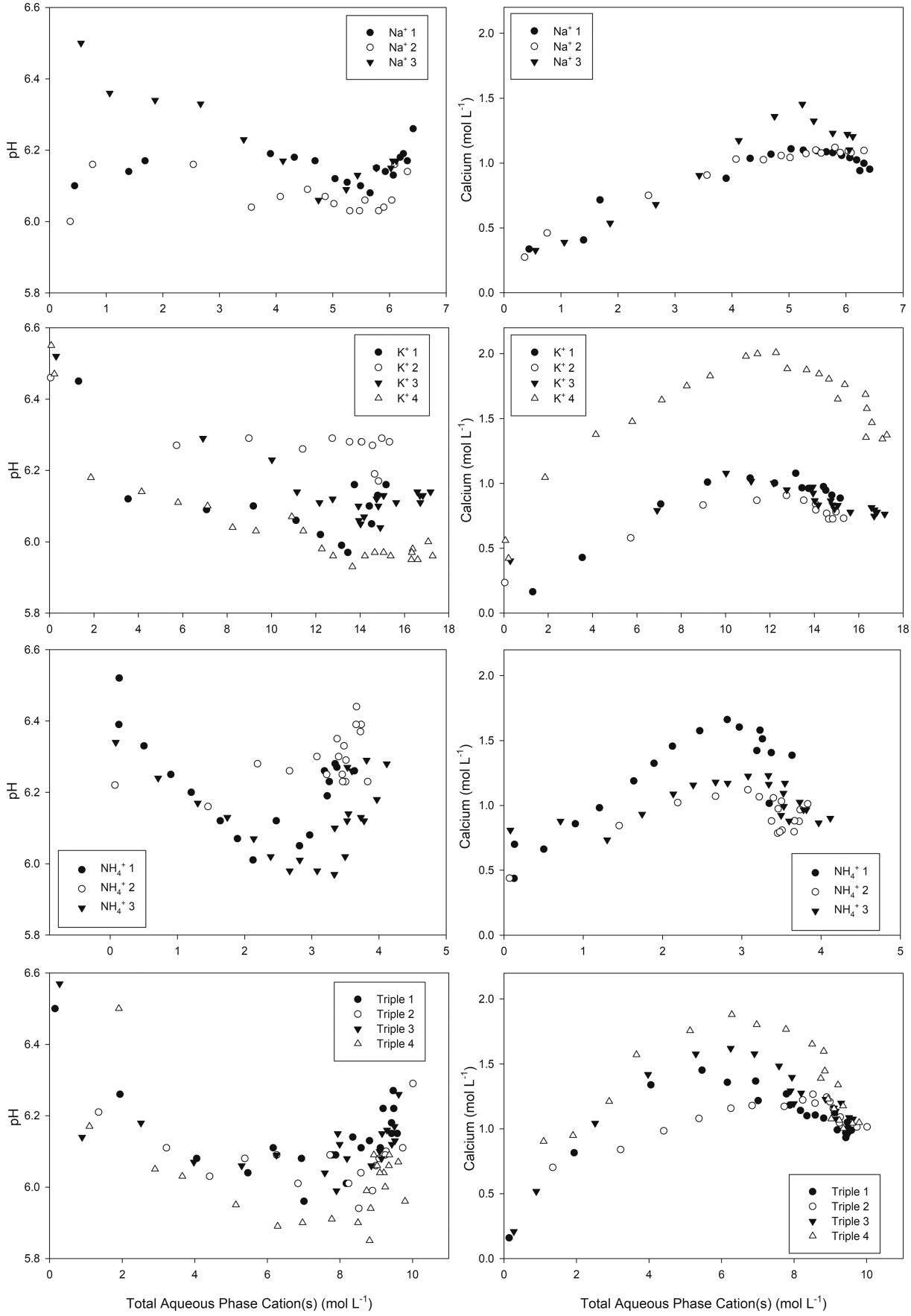
pH
Calcium (mol L-1)
Na+ 1
Na+ 2
Na+ 3
K+ 1
K+ 2
K+ 3
K+ 4
NH4+ 1
NH4+ 2
NH4+ 3
Triple 1
Triple 2
Triple 3
Triple 4
Total Aqueous Phase Cation(s) (mol L-1)

Figure 8

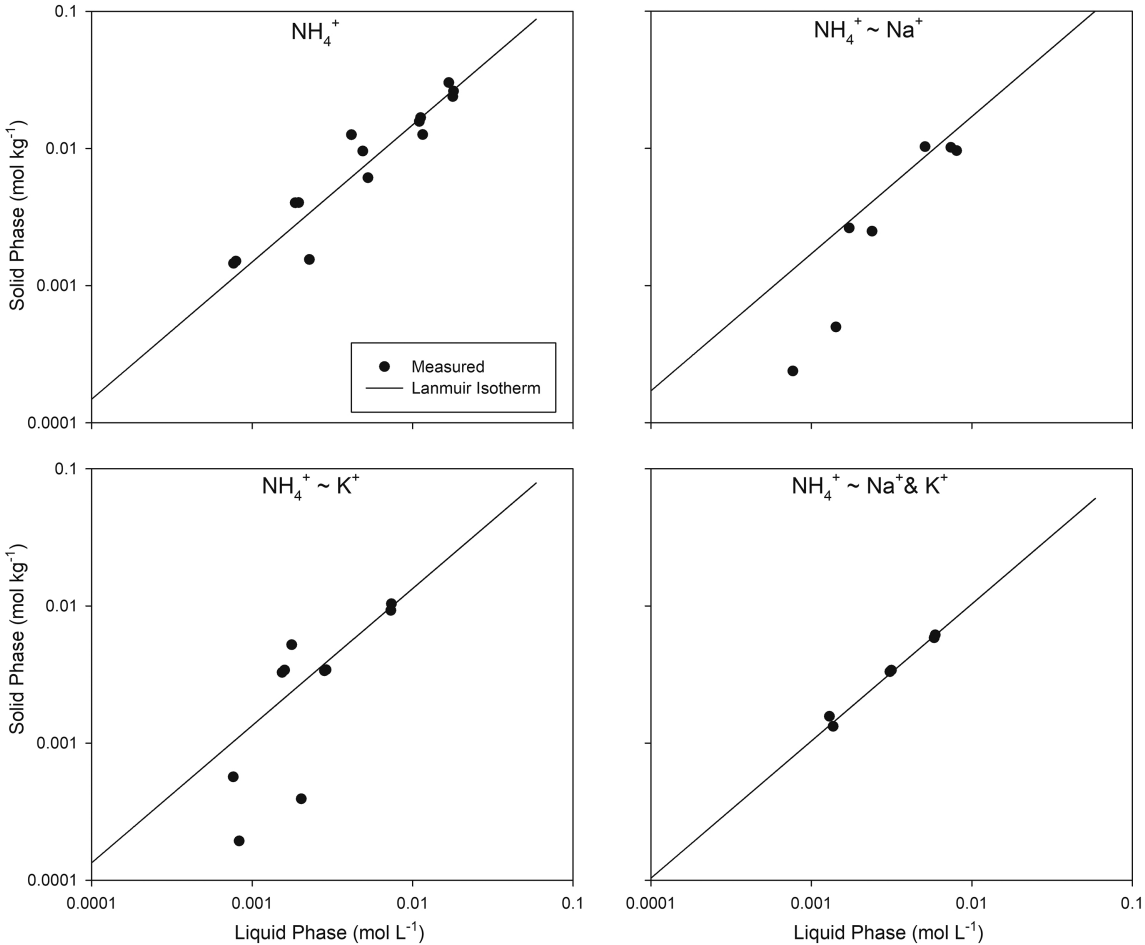
NH4+
NH4+ ~ Na+
NH4+ ~ K+
NH4+ ~ Na+& K+
Measured
Lanmuir Isotherm
Solid Phase (mol kg-1)
Liquid Phase (mol L-1)
0.1
0.01
0.001
0.0001

Figure 9